

4. GPIIb/IIIa receptor targeted rutin loaded liposomes for site-specific antithrombotic effect

4.1 Objective

The objective of this research was to prepare rutin loaded non-targeted and targeted anti-thrombotic nanomedicines and to evaluate their physicochemical features, such as shape, particle size, and zeta-potential, *in-vitro* characteristics such as encapsulation, drug release, hemolysis, and entrapment efficiency, targeting capability, platelet binding fluorescence imaging study, blood clot assay, and *in-vivo* characterization such as tail bleeding, clotting time, FeCl₃ induced thrombosis model, pharmacokinetic study, and histopathology study.

4.2 Plan of study

- a. Preparation and optimization of rutin loaded non-targeted liposomes by ethanol injection method
- b. Preparation of rutin loaded GP IIb/IIIa receptor targeted liposomes
- c. Physicochemical and *in-vitro* evaluation of non-targeted and (RGD or ABX) targeted liposomes
 - Particle size, polydispersity index and zeta potential by DLS
 - Determination of encapsulation efficiency
 - Electron microscopy (SEM, TEM & SAED)
 - Degree of peptide conjugation by Bradford Assay
 - Surface chemistry by XPS
 - Crystallographic studies by XRD
 - Physical stability by TGA
 - *In-vitro* drug release studies
 - *In-vitro* blood clot assay
 - *In-vitro* coagulation aPTT and PT assay
 - Platelet aggregation study

- Biocompatibility and safety evaluation
- *In-vitro* cytotoxicity assay
- *In-vitro* clot targeting efficiency by platelet binding
- Stability studies

d. *In-vivo* evaluation of non-targeted and targeted liposomes

- Tail bleeding assay in Swiss Albino mice
- Blood clotting time study in Swiss Albino mice
- FeCl₃ induced thrombosis model
- Pharmacokinetic studies in Sprague Dawley rats
- Histopathology studies on Sprague Dawley rats

4.3. Material

Rutin, N-hydroxysuccinimide, and 1-(3 dimethylaminopropyl)-3-ethylcarbodiimide hydrochloride were procured from Sisco Research Laboratories Pvt. Ltd., Mumbai, India. Arg Gly-Asp (RGD) peptide, thrombin, fibrinogen, and D- α -tocopheryl polyethylene glycol 1000 succinate (TPGS) were purchased from Sigma-Aldrich (St. Louis, MO, USA). Hydrogenated phosphatidylcholine from soyabean (HSPC) was a generous gift from Lipoid GmbH, Germany. Phospholine ES and phosphoplastin RL were generous gifts provided by R2 Diagnostic Inc., Indiana, USA. Abciximab injection was purchased from Reliance Life Sciences Pvt. Ltd., Navi Mumbai, India. Ferric chloride was purchased from Thermo Fischer Scientific India Pvt. Ltd., Mumbai, India. Calcium chloride and cholesterol were obtained from Central Drug House (P) Ltd., New Delhi, India. Fetal bovine serum (FBS) was procured from Gibco Life Technologies (AG, Switzerland). All solvents such as dichloromethane (DCM) and ethanol were of HPLC grade. Millipore water was produced by the LAB-JAL Milli-Q system (Lab India Instrument Pvt. Ltd.).

4.4. Methods

4.4.1. Selection of CMAs and CQAs

Preliminary studies were conducted to identify the important quality attributes of the generated system on the basis of the required quality product profile. Particle size was selected as one of the Critical Quality Attributes (CQAs) because a smaller size enhances the surface area and is capable to avoid the RES uptake. Entrapment efficiency was an additional CQA that was chosen because it is typically responsible for drug loading that is subsequently needed for therapeutic action. The PDI was further selected as a CQA because the monodispersity of particles can later decide the fate of drug release. Critical Material Attributes (CMAs) were also selected among several material attributes based on a literature survey [175].

4.4.1.1. Formulation optimization by Box-Behnken design (Randomized)

Numerical and graphical optimization of the liposomal formulation was performed to establish an optimized batch by using the Box-Behnken design. Cholesterol concentration (24-48 mg), HSPC concentration (49-98 mg), and TPGS concentration (14-42 mg) were used as independent variables to study the effect on formulation characteristics, i.e., particle size, PDI, and %EE (response variable), during the optimization of the formulation as shown in **Table 4.1**. There were a total of 15 batches in the design space representing 3 center points and 12 axial points mentioned in **Table 4.3**.

Table 4.1. Box-Behnken design of liposomes explaining different variables

Independent variables	Levels		
	-1	0	+1
X1= Weight of cholesterol (mg)	24.0	36.0	48.0
X2= Weight of HSPC (mg)	49.0	73.5	98.0
X3= Weight of TPGS (mg)	14.0	28.0	42.0
Dependent variables or Response	Constraints		

Y1= Particle size	Minimize
Y2= PDI	Minimize
Y3=Encapsulation efficiency	Maximize

4.4.2. Fabrication of nontargeted and (RGD or ABX) targeted liposomes

For the fabrication of nontargeted and targeted liposomes, the antithrombotic drug RUT was loaded in TPGS and TPGS-COOH modified liposomes prepared by ethanol injection method with slight modification [201]. In brief, RUT, HSPC, cholesterol, TPGS, or TPGS-COOH was dissolved in ethanol in a separate container. Moreover, the aqueous phase was heated (PBS 7.4 pH) at 60 °C with vigorous stirring in a beaker. The preheated ethanolic phase was then added to the aqueous phase in a dropwise manner. The temperature was maintained at 60 °C throughout the preparation process. After the complete removal of organic solvents, the formation of RUT loaded multilamellar liposomal vesicles occurs. The fabricated liposomes were large in size, so it was further reduced by probe sonication (Hielscher, Germany) for 4 min [165]. The vortexing was also used for a few minutes to make a homogeneous suspension of liposomes. Finally, liposomes were centrifuged to remove the untrapped drug from liposomes and were stored at 4 °C. Targeted liposomes were prepared by the same methodologies with additional steps. Briefly, 14 mg of TPGS was replaced with TPGS-COOH, and after formulating TPGS-COOH coated liposomes, they were post decorated with targeting ligands such as RGD or ABX by using carbodiimide chemistry. An equimolar amount of EDC and NHS was added for activation of the carboxylic group present on liposomes, and then targeting agents (RGD or ABX) were attached on the surface [172]. The blank liposomal formulations were prepared by the same procedure without incorporating RUT. The scheme of formulating liposomal vesicles and RGD-RUT-LIPO liposomes or ABX-RUT-LIPO liposomes has been presented in

Figure 4.1 A and Figure 4.1B, respectively, and the different constituents of liposomal batches have been provided in Table 4.2.

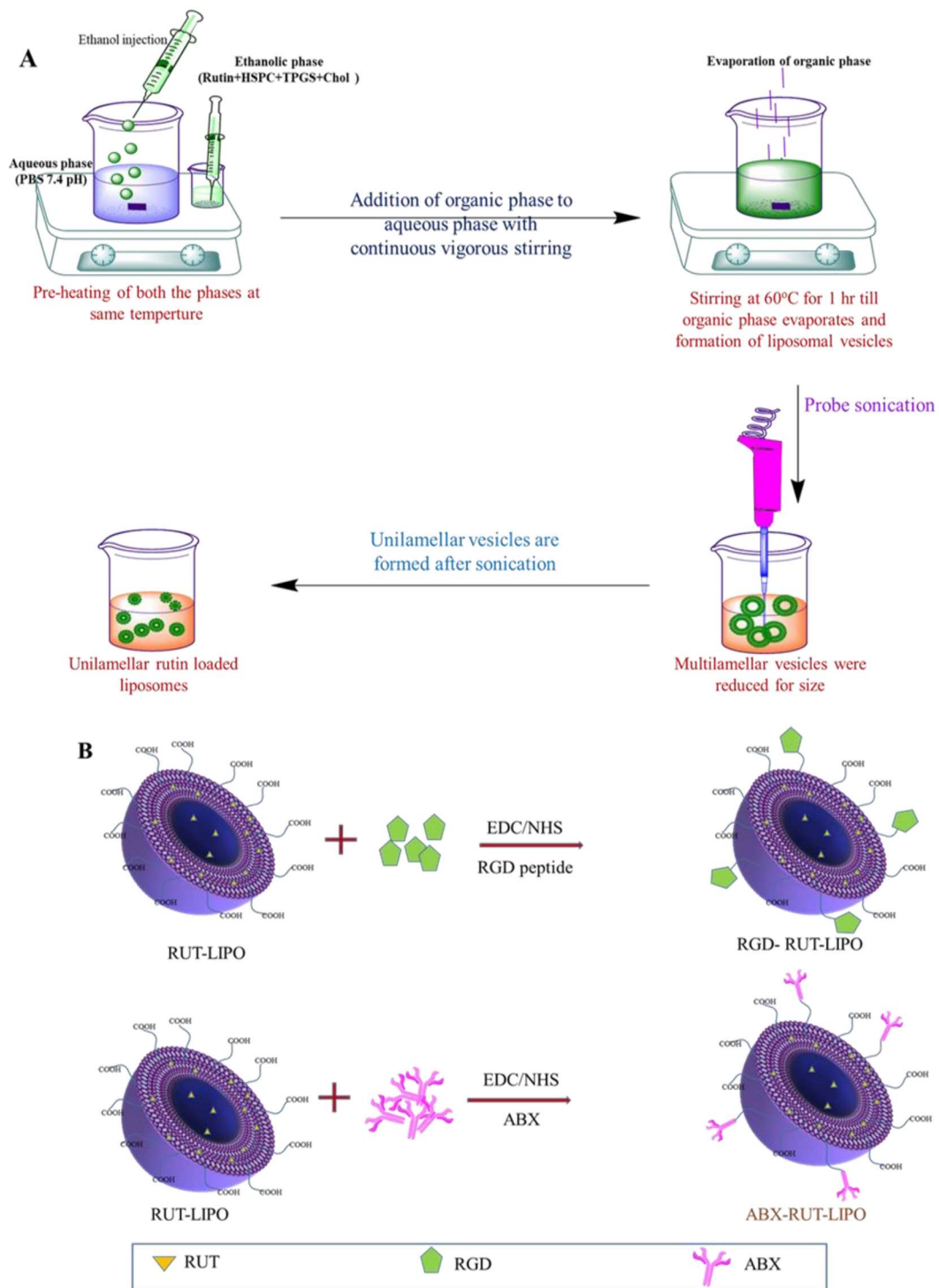


Figure 4.1. (A) Schematic representation of synthesis of RUT-LIPO and (B) RGD or ABX conjugation on RUT-LIPO

Table 4.2. Composition formulas of liposomal preparations

Batches	HSPC (mg)	Cholesterol (mg)	TPGS (mg)	TPGS- COOH (mg)	RUT (mg)	DiD Dye (µg)
RUT-LIPO	98	48	28	----	5	----
RGD-RUT-LIPO	98	48	14	14	5	----
ABX-RUT-LIPO	98	48	14	14	5	----
DiD-LIPO	98	48	28	----	----	200
RGD-DiD-LIPO	98	48	14	14	----	200
ABX-DiD-LIPO	98	48	14	14	----	200

4.4.3. Preparation of dye loaded liposomes

The liposomes were prepared by the ethanol injection method, the same as mentioned above. In brief, 200 µL of solution of DiD dye (1 mg/mL in DMSO) was added to 0.5 mL of ethanol, containing HSPC, cholesterol, TPGS, and TPGS-COOH. The preheated ethanolic phase was then added to the aqueous phase in a dropwise manner. During the preparation, the temperature was maintained at 60 °C as shown in **Figure 4.1A**. After that, the entire solution was ultrasonicated for 4 min by using a probe sonicator. Then obtained liposomes (DiD-LIPO) were filtered using a 0.22 µm filter and checked for physical characteristics [201]. Furthermore, dye loaded targeted liposomes were prepared with the same above-mentioned method.

4.4.4. Evaluation of prepared liposomes for their physicochemical characteristics

4.4.4.1. Particle size and polydispersity index (PI) determination

Particle size and polydispersity index were determined by a particle size analyzer (Malvern Zetasizer S90, U.K.) that works on the principle of dynamic light scattering. The measurement was taken with 10 times dilution of liposomal suspension in Millipore water. All the measurements were performed in triplicate at room temperature [179].

4.4.4.2. ζ Potential measurement

The ζ potential of liposomes was measured by zetasizer (Malvern Zetasizer Pro, U.K.). Samples were diluted 10 times with the aqueous phase of the formulation, and the measurement was carried out to get the surface charge on liposomes which influences the stability of the formulations [180].

4.4.4.3. Encapsulation efficiency

Drug-loaded nontargeted and targeted liposomes were ruptured in the organic solvent (methanol) system under bath sonication for 3 h at room temperature. The solution was filtered through a 0.22 μm syringe filter, and absorbance was determined at $\lambda_{\text{max}} = 360$ nm using UV spectroscopy [202]. Encapsulation efficiency was calculated as indicated below:

$$\text{Encapsulation (\%)} = (\text{Amount of drug entrapped}/\text{Amount of drug added}) \times 100$$

4.4.4.4. Scanning electron microscopy (SEM)

Surface morphology of the RUT-LIPO, RGD-RUT-LIPO, and ABX-RUT-LIPO was captured by using a scanning electron microscope (Nova Nano SEM 450, USA (S.E.A.) PTE, Ltd.) at room temperature. 10 times diluted liposomal samples were casted on the separate coverslip and spread uniformly to get the uniform thin film. After, overnight drying of the samples was done under a vacuum, and carbon coated liposome images were captured at a magnification of 20 kV and 50 KX [181].

4.4.4.5. Transmission electron microscopy (TEM)

The surface morphology (particle size and the shape of the liposomes) and architecture of the prepared nontargeted and targeted liposomes were explored using transmission electron microscopy (Tecnai G2 20 TWIN, FEI Company, USA). The samples were diluted 10 times and bath sonicated for 5 min to mix uniformly. A drop of each sample was placed on

a copper TEM grid separately and dried overnight under a vacuum before they were subjected to imaging [180].

4.4.4.6. Degree of peptide conjugation by Bradford assay

The dilution of bovine serum albumin (BSA) was prepared to make a standard calibration curve. The aliquot from 1 mg/mL BSA solution was withdrawn to produce the required dilutions (6.25, 12.5, 25, 50, 100, and 200 μ L), and further PBS was added to make up the volume to 1000 μ L in an Eppendorf tube. Micropipettes were used to make dilutions with precision. The targeted liposomal suspensions were then diluted (10 \times , 50 \times , 100 \times) and standard ABX/RGD solutions (same dilutions) were added to the microwell in a 96-well plate in a triplicate manner. The volume of sample added in each microwell was 10 μ L with 250 μ L of Bradford reagent. The plate was incubated in the dark at room temperature for 15 min. Last, the appeared color of the solutions was detected by a microplate reader at $\lambda_{\text{max}} = 595 \text{ nm}$ [171, 174].

4.4.4.7. Surface chemistry

X-ray photoelectron spectroscopy (XPS, K-Alpha, Thermo Fisher Scientific) was used to examine the surface chemistry of nontargeted and targeted liposomes at a binding energy of 200–800 eV. A drop casting of the liposomal suspension was performed on a 1 cm \times 1 cm glass slide and dried overnight under the vacuum dryer. The obtained samples were investigated for XPS analysis [203].

4.4.4.8. X-ray diffraction (XRD) analysis

It was used to check changes in the crystallinity and physical state of the drug after encapsulation and to study the physical properties of the drug and excipients in pure form and nanoform. An X-ray diffractometer (Rigaku Miniflex 600 desktop X-ray diffraction system, Japan) was used to obtain the XRD spectra of RUT and optimized liposomal formulations. The diffractograms were captured using a Ni-filtered Cu K α 1 X-ray radiation

source, 15 mA amperage, 40 kV tube voltage, $10^{\circ} \text{ min}^{-1}$ scan rate, 0.02° step size, and a scanning range of $20\text{--}80^{\circ}$ angle of 2θ [204].

4.4.4.9. Thermogravimetric analysis (TGA)

The thermal stability and decomposition of RUT, cholesterol, TPGS, HSPC, and liposomal formulation (RUT-LIPO) were determined by using TGA (Shimadzu, Japan). The weight of all the samples was in the range of 2–3 mg in dried form. TGA data of all prepared samples were collected at a heating range of $25\text{--}500^{\circ} \text{ C}$. The standard flow rate of N_2 was maintained during the experiment, and the heating increment rate was at $10^{\circ} \text{ C}/\text{min}$ [205].

4.4.5. In-vitro studies

4.4.5.1. In-vitro drug release study

The dialysis bag diffusion method was used for the in vitro drug release study of RUT and RUT loaded nontargeted and targeted liposomes. Each liposomal suspension containing 5 mg of RUT was kept in a 1 kDa dialysis bag and sealed with a dialysis clip to avoid any leakage. Then this dialysis bag was dipped in 100 mL of PBS, pH 7.4. The system was kept at $37 \pm 0.5^{\circ} \text{ C}$ with gentle stirring (IKA C-MAG HS-7). The samples (3 mL) were withdrawn at a predetermined sampling interval, and an equal volume was replenished with release media (PBS, pH 7.4). The amount of drug released was determined by analyzing the obtained samples under UV spectroscopy [206].

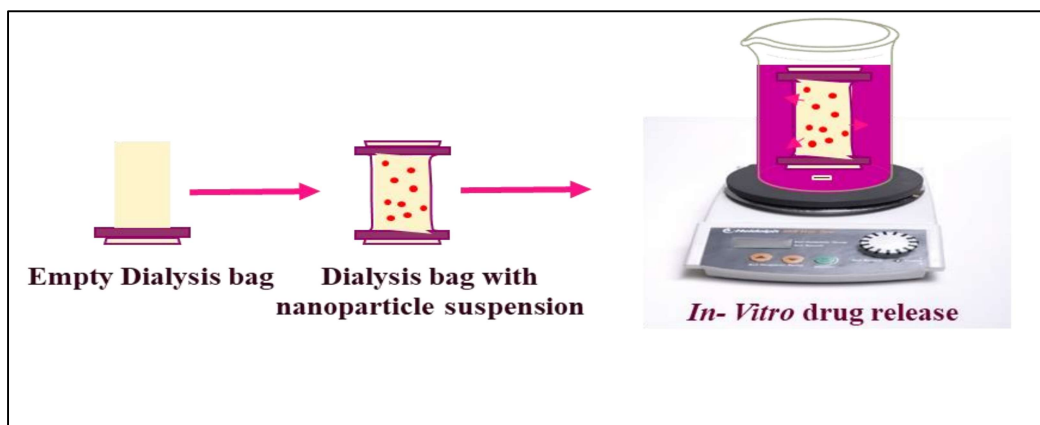


Figure 4.2. Graphical representation of drug release study by dialysis bag method

4.4.5.2. Blood clot analysis

This study was carried out according to an earlier report with some modifications. The blood samples (800 μL) were obtained from vein puncture of healthy human volunteers and were immediately mixed with 200 μL of saline, blank liposomes with RGD conjugation (BLNRGD- LIPO), blank liposomes with ABX conjugation (BLN-ABX- LIPO), RUT (positive control), RUT-LIPO, RGD-RUTLIPO, and ABX-RUT-LIPO liposomes. Then it was incubated for 1 h at 37 $^{\circ}\text{C}$ and clot weight was measured and compared. The concentration of RUT in each sample was kept equal (1 mg/mL), and for blank formulation volume was kept equal to get a related antithrombotic effect [207].

4.4.5.3. In vitro coagulation aPTT and PT assay

Briefly, plasma was separated from the blood obtained from healthy humans in citrate coated tubes by centrifugation. After that, equal amounts of drug containing nontargeted and targeted liposomes (200 μL) were subjected for incubation with collected plasma (200 μL) for 3 min. 100 μL of control or test plasma was used in the case of PT assay and mixed with the same volume of PT reagent (Phosphoplastin RL). However, in the case of aPTT assay, 50 μL of plasma was used and mixed with aPTT reagent (Phospholin ES) and calcium chloride (0.25 M). All the reagents used in this study were warmed at 37 $^{\circ}\text{C}$. The saline was taken as negative control, and RUT was taken as a positive control. Finally, the activated partial thromboplastin time (aPTT) and prothrombin time (PT) were determined by a coagulometer (Diagnostica Stago, France) [12, 208]. The method of PT and aPTT assay had been presented in **Figure 4.3**.

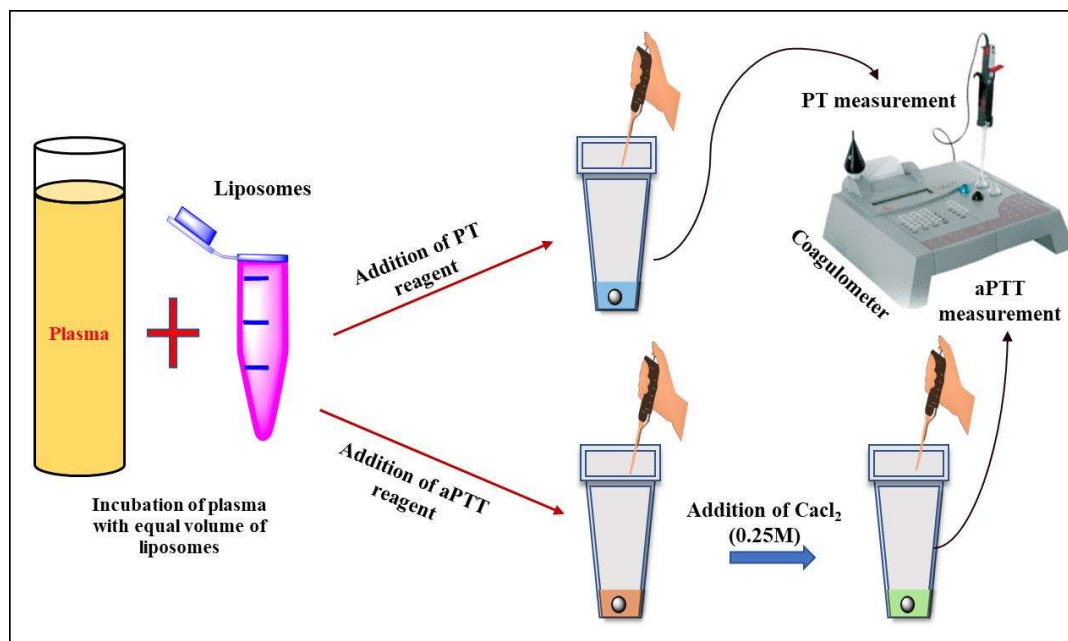


Figure 4.3. Graphical representation of method for PT and aPTT assay

4.4.5.4. Platelet aggregation study

The turbidimetry method was used to perform a platelet aggregation assay with the help of SpectraMax M5 multimode microplate reader (Molecular Devices LLC, USA) [209]. Human blood samples were collected from a healthy adult volunteer using Dispo Van syringe and collected in citrate coated tubes to avoid coagulation. Then it was centrifuged at 350 x g for 20 min to separate platelet-rich plasma, then centrifuged again at 1450 x g to form pellet the platelets. The sedimented platelets were washed one more time with physiological saline. The final pellet was resuspended in the platelet-poor plasma (PPP) and adjusted to a final platelet concentration of approximately 2×10^8 cells/mL as counted by a hemocytometer. Then 100 μ L of 1 mg/mL concentrations of RUT, RUT-LIPO, RGD-RUT-LIPO, and ABX-RUT-LIPO was incubated with the platelet rich plasma for 4 min before the addition of fibrinogen and thrombin. Blank formulations, i.e., BLN-RGD-LIPO and BLN-ABX-LIPO, were also taken as control at same volume. The maximum agglomeration (MAR) was evaluated by the percentage of maximum increase in light

transmission. PPP showed 100% transmission [210]. The method of platelet aggregation study had been presented in **Figure 4.4**.

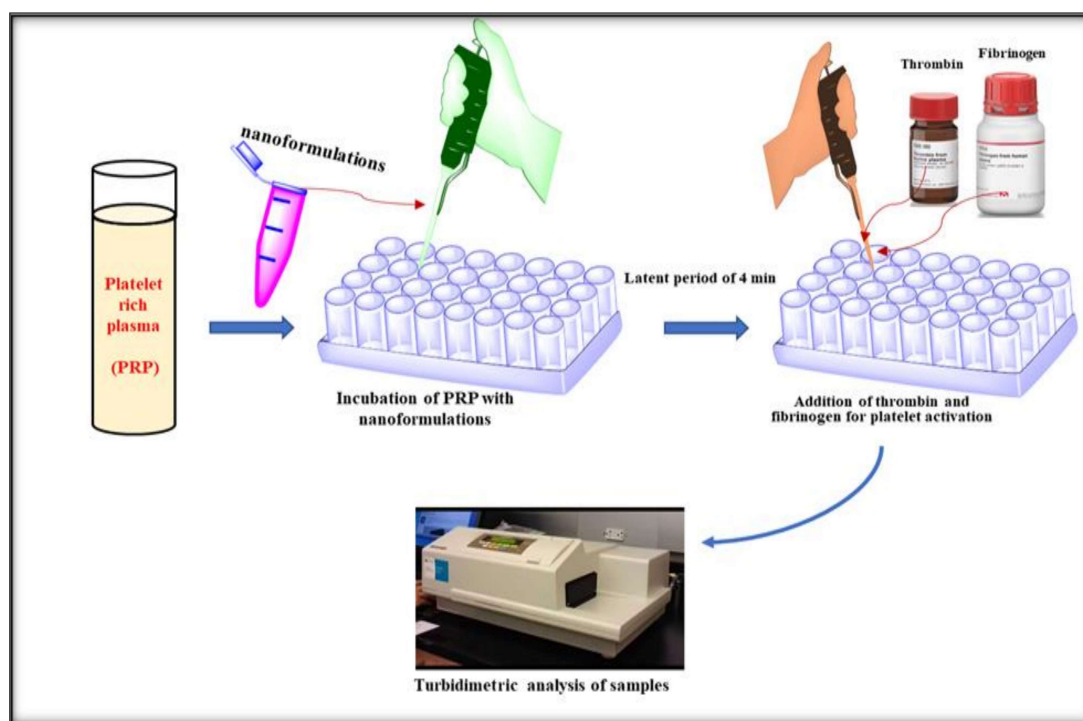


Figure 4.4. Graphical representation of a method for platelet aggregation study

4.4.5.5. Biocompatibility and safety evaluation

4.4.5.5.1. Blood smear analysis

A blood smear study was performed to analyze the morphological changes in blood components. A vein puncture was used to collect blood (5 mL) from a healthy human volunteer in a 3.8% sodium citrate solution (9:1 ratio). The 200 μL of standard RUT solution saline and each liposomal formulation in the same concentration (1 mg/mL) were mixed with 800 μL of collected blood. This mixture was kept at 4 $^{\circ}\text{C}$ for 24 h. After that, a drop was cast as a smear of the resultant blood mixtures. The prepared smears of the all samples were stained with Wright-Giemsa stain and sequentially washed with isotonic buffer solution. The blood smear samples were then air-dried and observed under a bright field microscope [12].

4.4.5.5.2. Hemolytic assay

The biocompatibility of liposomal formulations was checked by hemolysis assay. Hemolysis with less than 10% was considered safe. Blood was collected from the healthy human volunteers and centrifuged for 15 min at 825 x g to segregate the red blood cells (RBCs). The supernatant was removed, and the RBCs as sediment were washed with PBS thrice. The 2% v/v solution of RBCs in PBS was prepared, and 100 μ L of this solution was incubated with 100 μ L of each liposomal formulation (1 mg/mL RUT concentration) including 800 μ L of saline as a diluent. The mixture was incubated for 1 h at 37 °C and centrifuged at 825 x g for 5 min. The supernatant (200 μ L) was transferred to a 96-well plate. PBS (0.01 M, pH 7.4) and 1% Triton X were taken as a negative and positive controls, respectively, with RBCs solution in the same quantity (100 μ L). The absorbance was taken by a microplate reader at 540 nm. The % hemolysis was computed according to the following equation [211].

$$\begin{aligned} & \% \text{ hemolysis} \\ &= \frac{\text{absorbance of test sample} - \text{absorbance of PBS sample}}{\text{absorbance of Triton X sample} - \text{absorbance of PBS sample}} \times 100 \end{aligned}$$

4.4.5.6. In-vitro cytotoxicity assay

The mouse fibroblast L929 cell line was cultured in Dulbecco's modified Eagle's medium (DMEM; containing 10% of FBS) and was incubated in a humidified incubator (with 5% CO₂) at 37 °C. The cytotoxicity of RUT, RUT-LIPO, RGD-RUT-LIPO, ABXRUT-LIPO, BLN-LIPO, BLN-RGD-LIPO, and BLN-ABXLIPO was assessed by MTT assay using L929 cells as a model. Briefly, L929 cells were seeded in 96-well culture plate by keeping cell count (5000 cells per well) and cultured overnight to allow proper cell adhesion. Then, all the samples with different concentrations of RUT (100, 50, 25, 12.5 μ g/mL) were prepared by serial dilution with culture media and was added to the microwell in triplicate manner. After 48 h of incubation the culture medium of the 96-well plate was replaced with

100 μ L of 10% MTT solution in DMEM. After 4 h of incubation with MTT solution, it was replaced with 100 μ L of DMSO and shaking was allowed for half an hour. Finally, the absorbance was measured by microplate reader at 570 nm wavelength [193]. The % cell viability was then calculated using the below equation:

$$\% \text{ cell viability} = \frac{\text{absorbance of test sample}}{\text{absorbance of control}} \times 100$$

4.4.5.7. *In vitro* clot targeting efficiency by platelet binding

4.4.5.7.1. *In vitro* imaging

A fluorescent imaging system (Photon Imager Optima, Biospace Lab, France) was used to determine *in-vitro* clot targeting efficiency of targeted liposomes to activated platelets. For this study DiD dye loaded nontargeted and targeted liposomes were prepared and an excess of unloaded dye was extracted by centrifugation at 125 x g for 30 min. The platelets were isolated from human blood, and washing was carried out with a saline solution. Further, platelets were resuspended in the original volume of saline and transferred to the glass vials. As for the platelet activation, 10 μ L of 10 U/mL of thrombin with 20 μ L of 10 mg/mL fibrinogen was added to the vials. Concurrently, DiD dye, DiD-LIPO, RGD-conjugated DiD loaded liposomes (RGD-DiD-LIPO), and ABX-conjugated DiD loaded liposomes (ABX-DiD-LIPO) were transferred to the vials and allowed to incubate for 1 h. Afterward, the prepared mixture was centrifuged for 20 min at 3250 x g and the supernatant was drawn out. The obtained platelets were resuspended in phosphate buffer saline (pH 7.4) and were visualized under the imaging system. The fluorescent signals (region of interest, ROI) of control and test samples were collected and compared. All vials contained an equivalent amount of DiD dye, and the instrument was set at 550 nm emission wavelength and 575 nm excitation wavelength [189] [212].

4.4.5.7.2. ImageJ analysis of confocal laser scanning microscopy (CLSM) images

The DiD dye loaded liposomes (DiD-LIPO, RGD-DiD-LIPO, and ABX-DiD-LIPO, 100 μL) were incubated with activated platelets (3×10^7) for an hour followed by fixing of the cells utilizing 4% v/v paraformaldehyde solution. The washing of the cells was performed thrice to remove excess non-interacted liposomes with pH 7.4 PBS. The in vitro clot targeting efficacy was determined by measuring the amount of red channels of obtained CLSM by ImageJ software. The images were converted to binary black and white picture by ImageJ and quantified for the dark area as it signifies the red channel intensity in fluorescent images that estimates the affinity of DiD-LIPO, RGD-DiD-LIPO, and ABX-DiD-LIPO toward activated platelets [190] [213].

4.4.5.8. Stability studies

4.4.5.8.1. Stability study in serum

The serum stability of RUT-LIPO in 10% v/v fetal bovine serum (FBS) was determined by particle size analysis. The liposomal suspension was added with 10% v/v FBS and incubated for 3 days in the dark. The particle size of liposomes was analyzed before and after the incubation [193].

4.4.5.8.2. Storage stability study

The nontargeted and targeted liposomes were prepared and checked for particle size after 10 times dilution with PBS pH 7.4. Then the sample was stored at 4–8 °C for 3 months. After the given time interval (3 months), the size of the liposomal formulations was examined to determine stability [214].

4.4.6. In-vivo studies

4.4.6.1. Tail bleeding assay

Measurement of bleeding time in animals is mainly done for the evaluation of hemorrhagic characteristics of antithrombotic drugs. Twenty male Swiss albino mice weighing about 20

± 2 g were selected for the study and divided into 7 groups ($n = 5$). The age of the selected animals was 5–7 weeks. The saline, BLN-RGD-LIPO, BLN-ABX-LIPO, RUT, RUT-LIPO, RGD-RUT-LIPO, and ABX-RUT-LIPO liposomal suspensions were administered (500 $\mu\text{g}/\text{kg}$ of RUT) by tail vein injection. The higher dose of these potent liposomes might cause bleeding; thus a lower dose of 500 $\mu\text{g}/\text{kg}$ was selected for this study. The concentration of RUT was similar in all the batches of nontargeted and targeted liposomes. As for blank formulation, the volume was kept equal. Further, the mice were anesthetized and kept on the heating table (37 °C) in the supine position. After completion of the latent period (1 h), the tail of the mice was transected with the surgical blade at a 1 cm distance from the tail tip. Instantly, after transection, the tail was dipped in the tube filled with saline (50 mL). The time was recorded up to the time until the bleeding stopped and was noted as bleeding time. The maximum observation was done for 400 sec [192, 193].

4.4.6.2. Blood clotting time study

Measurement of blood clotting time was performed as reported earlier. Briefly, the saline, RUT, RUT-LIPO, RGD-RUT-LIPO, ABX-RUT-LIPO, BLN-RGD-LIPO, and BLN-ABX-LIPO were administered at a dose of 500 $\mu\text{g}/\text{kg}$ of RUT (equal volumes of blank formulations were used) through tail vein. The tail of the mice was transected at the tip with the help of a surgical blade after 1 h of i.v. administration. The 25 μL of blood was collected in a microhematocrit capillary tube. The blood flow was allowed within the capillary by tilting it at an angle of 60° in up and down directions. The stopwatch was started at the point of blood contact with capillary tube. The clotting time was reported as the blood ceased to flow in the capillary with the horizontal plane [194].

4.4.6.3. In-vivo FeCl_3 model for thrombus formation by B.P measurement

Male Sprague Dawley rats weighing about 200 ± 20 g were kept in the animal house at room temperature of 25 ± 2 °C. Food and water were provided ad libitum (Hindustan Liver

Ltd.). A modified version of blood pressure measurement was used in which invasive direct BP was recorded [195]. Rats were anesthetized by ip injection of urethane (1.5 g/kg) and placed on a heat controllable table to prevent hypothermia. The midline cervical incision was performed to expose the carotid artery and was separated from the vagus nerve. Later, proximal cannulation of the carotid artery was performed for the direct measurement of blood pressure by PowerLab, AD Instruments, Australia. The intravenous tail vein injection of saline, BLN-RGD-LIPO, BLNABX- LIPO, RUT, RUT-LIPO, RGD-RUT-LIPO, and ABX-RUT-LIPO at a dose of 5 mg/kg of RUT was administered to the anesthetized rat. As for the blank formulation, a similar volume was taken as other formulations. Thrombosis was induced after 2 h of the injection by the topical treatment of FeCl₃ (20% w/v) soaked with Whatman filter paper (2 mm × 1 mm) to the same carotid artery in front of the cannulation point. Before the FeCl₃ application, normal blood pressure was recorded for at least 10 min as the initial recording. Aluminum foil was kept below the artery to avoid the contact of FeCl₃ with other tissues, before the application. The time for cessation in blood flow after the application of FeCl₃ was noted [196]. After the treatment of the carotid artery with FeCl₃, the cessation in blood flow and a 50% fall in blood pressure were determined as the end point of the study. The experiment was performed in the controlled environmental condition of a temperature of around 25 °C.

4.4.6.4. Pharmacokinetics study

Male Sprague Dawley rats weighing about 200 ± 20 g were taken for the pharmacokinetic study and kept in the animal house at room temperature 25 ± 2 °C. Food and water were provided ad libitum. The rats were categorized to the following treatment groups RUT, RUTLIPO, RGD-RUT-LIPO, and ABX-RUT-LIPO. Briefly, each formulation and drug solutions were diluted in PBS 7.4 and administered slowly to the tail vein at a dose of 5 mg/kg of RUT. After the administration of drug and formulations, blood samples were

withdrawn via retro-orbital plexus at 0.5, 1, 2, 4, 8, 12, 24, and 48 h time points in an Eppendorf containing 3.8% sodium citrate solution. Then all the collected samples were centrifuged at 5800 x g for 15 min to separate the plasma. The clear plasma (200 μ L) was then mixed with mobile phase (90 acetonitrile/10 methanol) in the ratio of 1:2 and was vortexed for 5 min. After that it was again centrifuged for 15 min at 5800 x g and the clear supernatant was transferred into vials. An aliquot of 10 μ L of each sample was injected onto the HPLC column, and recorded data were compared with the calibration curve. A graph of plasma drug concentration vs time was plotted for the determination of pharmacokinetics parameters of RUT in liposomal formulations. All the analytical parameters (selectivity, linearity, accuracy, precision, extraction efficiency, LOQ, and LOD) were validated except specificity as aim of this study was to determine only rutin but not related components. So they are not studied in this experiment due to the requirement of better detector sensitivity for multiple components estimation simultaneously [215] [216].

4.4.6.5. Toxicity assay (Histopathology study)

A toxicity study was performed to determine the side effects and mortality that occurs after treating with the nontargeted and targeted liposomal formulations. All the liposomal formulations were injected by iv bolus (5 mg/kg) into 20 rats, n = 4 (half male and half female). The saline-treated group was taken as a negative control, and RUT treated group was taken as a positive control. The observation was done for 14 days to check the acute and chronic toxicity after administration. Based on observation, the formulations were designated as safe or well tolerated [27] [60].

4.4.7. Statistical investigations

The GraphPad Prism software was used for all the statistical calculations, and acquired experimental data were expressed as the mean \pm standard deviation (SD) of 3 independent values. The degree of significance was denoted as ns ($p \geq 0.05$), * ($p < 0.05$), ** ($p < 0.01$),

and *** ($p < 0.001$). To calculate significant differences statistically, Tukey's multiple comparison tests (one-way analysis of variance) was used.

4.5. Results and discussion

4.5.1. Formulation optimization by Box-Behnken design

Table 4.3. Box-Behnken design table with the response values

Batch No.	Chol. (mg)	HSPC (mg)	TPGS (mL)	Particle Size (nm)	PDI	%EE
1	48	49	28	152.9	0.185	60.89
2	36	49	14	191.7	0.215	61.09
3	36	98	14	256.4	0.287	62.87
4	48	73.5	42	229.4	0.249	70.18
5	36	73.5	28	156.6	0.186	64.09
6	36	73.5	28	156.0	0.185	64.09
7	36	73.5	28	134.7	0.163	64.09
8	24	98	28	132.0	0.157	44.54
9	24	49	28	135.9	0.184	33.23
10	24	73.5	14	218.6	0.248	40.31
11	36	98	42	176.4	0.200	72.93
12	48	98	28	192.9	0.218	70.62
13	36	49	42	215.5	0.224	43.89
14	48	73.5	14	243.0	0.274	50.06
15	24	73.5	42	168.8	0.186	08.81

4.5.1.1. Effect on particle size

For all the responses, the quadratic model was selected among various model i.e., linear, 2FI, and cubic. By considering the outcomes of statistical analysis of variance (ANOVA) of R^2 (0.9855), adjusted R^2 (0.9595), predicted R^2 (0.9518), and adeq precision (19.19), the model was analyzed. The predicted R^2 of 0.9518 is in reasonable agreement with the adjusted R^2 of 0.9595; i.e. the difference is less than 0.2. Adeq Precision measures the signal to noise ratio and indicates an adequate signal > 4 i.e., desirable. The results demonstrated

that the model fit was significant and the lack of fit was nonsignificant suggesting the suitability of the model. The relationship between the investigated factors and responses was depicted in **Figure 4.5** in terms of 2D contour plots and 3D surface plots. The polynomial equation generated by BBD showing the effect of different factors on particle size was given as follows:

$$Y_1 = 149.1 + 20.3625 A + 7.7125 B - 14.95 C + 10.975 AB + 9.05AC - 25.95BC + 4.6375 A^2 - 0.3125 B^2 + 61.2125 C^2$$

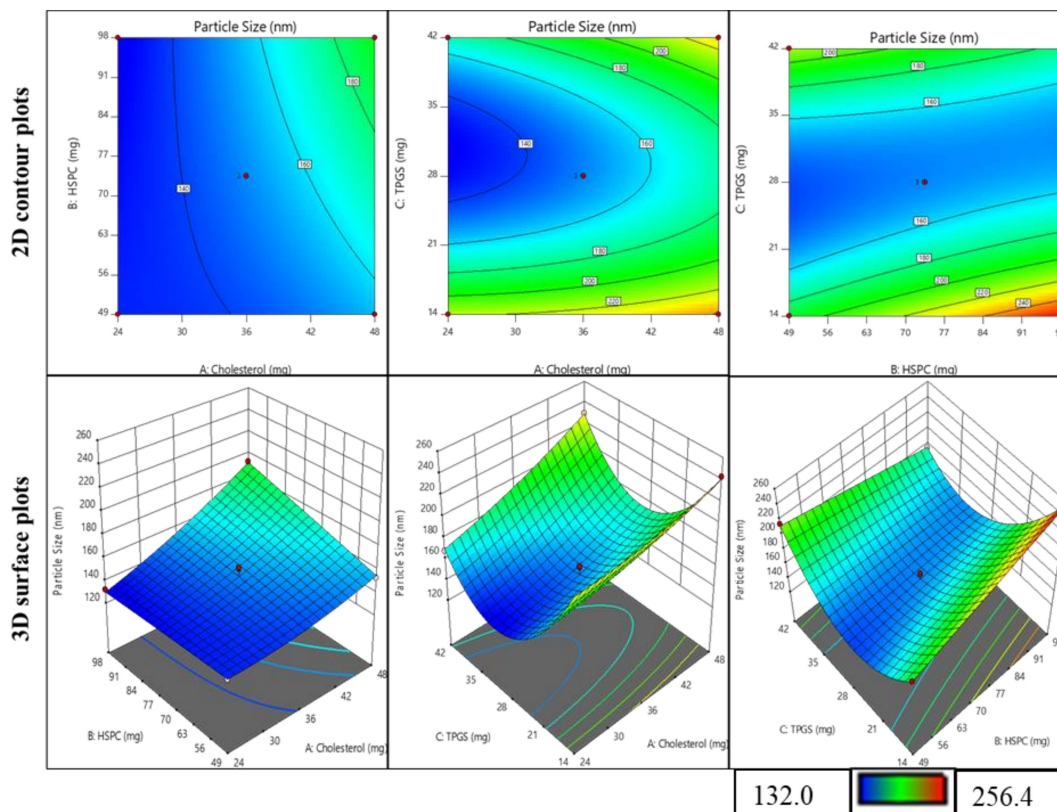


Figure 4.5. The 2D contour plots and 3D surface plots showing the effect of independent variables on particle size

4.5.1.2. Effect on PDI

The BBD study suggested a quadratic model as a best-fit model for the PDI optimization of nanoformulation. The statistical values were noted as R^2 (0.9693), adjusted R^2 (0.9139), predicted R^2 (0.7247), and adeq precision (13.22), after ANOVA analysis. The predicted R^2

of is in reasonable agreement with the adjusted R^2 with a difference of less than 0.2. Adeq precision values were > 4 as advisable. The results demonstrated that the model fit was significant and the lack of fit was nonsignificant suggesting the suitability of the model. The relationship between the investigated factors and responses was depicted in **Figure 4.6** in terms of 2D contour plots and 3D surface plots. The polynomial equation generated by BBD showing the effect of different factors on particle size was given as follows:

$$Y_2 = 0.178 + 0.018875 A + 0.00675 B - 0.020625 C + 0.015AB + 0.00925AC - 0.024BC + 0.007875 A^2 + 0.000125 B^2 + 0.053375 C^2$$

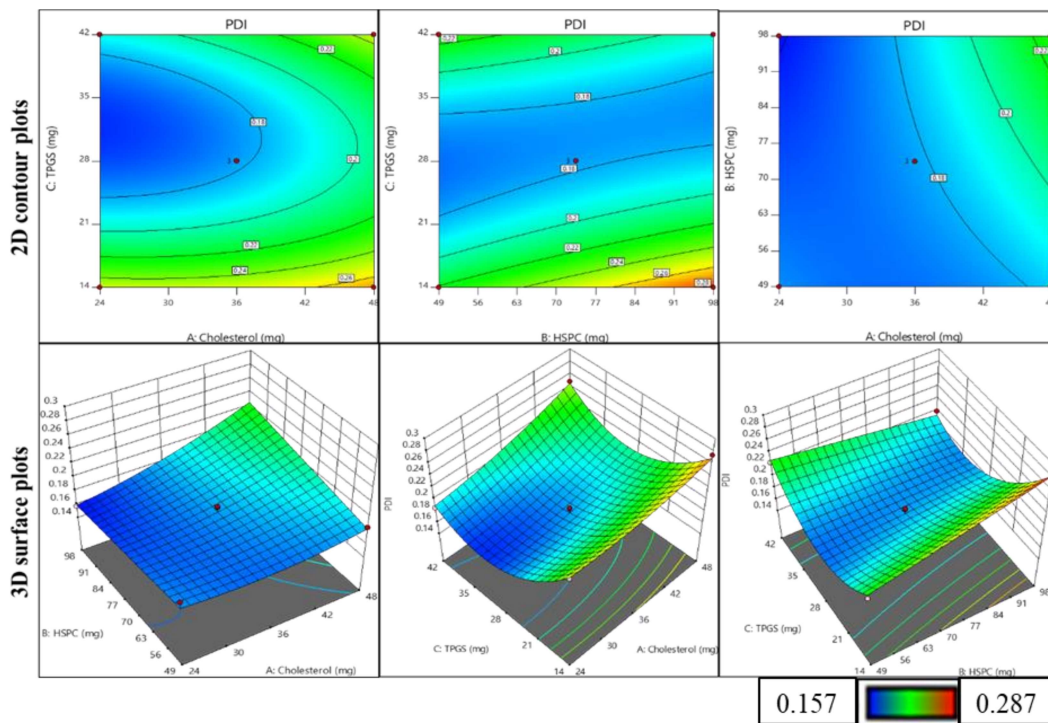


Figure 4.6. The 2D contour plots and 3D surface plots showing the effect of independent variables on PDI

4.5.1.3. Effect on %EE

The responses, of ANOVA, were noted as R^2 (0.9878), adjusted R^2 (0.9657), predicted R^2 (0.8042), and adeq precision (23.74), following quadratic model in case of EE. The predicted R^2 and adjusted R^2 showed a difference less than 0.2. and adeq precision value was > 4 suggesting the suitability of the model. The results demonstrated that the model fit

was significant and the lack of fit was nonsignificant suggesting the suitability of the model.

The relationship between the investigated factors and responses was depicted in **Figure 4.7** in terms of 2D contour plots and 3D surface plots. The polynomial equation generated by BBD showing the effect of different factors on particle size was given as follows:

$$Y_3 = 64.09 + 15.6075A + 6.4825B - 2.315C - 0.395AB + 12.905AC + 6.815BC - 14.8125A^2 + 3.0425B^2 - 6.9375C^2$$

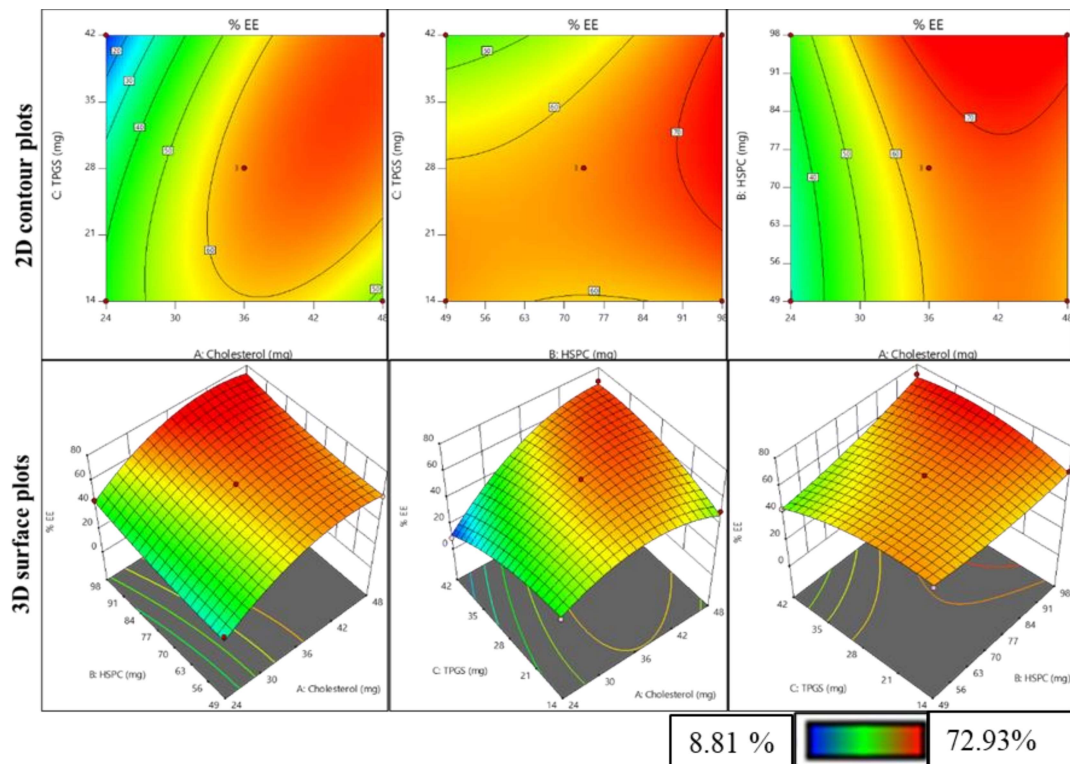


Figure 4.7. The 2D contour plots and 3D surface plots showing the effect of independent variables on %EE

The batch was selected by fixing the independent variables in the range. The response was set as a minimum for particle size, a minimum for PDI, and a maximum for %EE. The top 5 suggested batches were experimentally performed and compared with predicted data with a desirability of 1.00. According to experimental results, batch no. 12 was selected for further analysis.

4.5.2. Evaluation of prepared liposomes for their physicochemical characteristics

4.5.2.1. Particle size, PI, and ζ potential determination

The mean sizes of blank, RUT-LIPO, RGD-RUT-LIPO, and ABX-RUT-LIPO liposomes were 144.3 ± 3.48 , 194.1 ± 4.12 , 218.3 ± 2.45 , and 220.2 ± 3.54 nm, respectively (**Table 4.4**). The PI of all the optimized liposomal formulations was under 0.3. Moreover, the ζ potential values of blank, RUT-LIPO, RGD-RUT-LIPO, and ABX-RUT-LIPO liposomes were found to be -21.53 ± 0.71 , -22.68 ± 1.43 , and -23.67 ± 1.94 mV. The size of the liposomes is one of the crucial responses that should be closely observed considering the fact that later it eventually decides the fate (pharmaco-kinetics and dynamics) of the nanovesicles in the biological system. The results indicate an average size of the liposomes in the range of 100 to 300 nm. There was a notable increment ($P < 0.05$) in the size of targeted liposomes which might be caused by the incorporation of drug and surface conjugation of the peptide. The polydispersity index values of all the batches revealed a narrow size distribution and were found to be near about 0.3 (**Table 4.4**). The Zeta potential of nanoformulation confirms the binding of RGD and ABX as the zeta value shifted more to the negative side [217]. The presence of TPGS in the liposomal backbone prevents opsonization and enhances the biological half life of the nanoformulation [218].

4.5.2.2. Encapsulation efficiency

Percent encapsulation efficiency (%EE) was explained as the ratio of the amount of drug loaded into the liposomes to that of the total amount added during the preparation process. The %EE of the RUT-LIPO was found to be $70.93 \pm 5.86\%$. However, %EE of the RGD-RUT-LIPO and ABX-RUT-LIPO liposomes were 68.61 ± 7.65 , and $67.84 \pm 8.83\%$, respectively (**Table 4.4**). The impact of encapsulation efficiency was considered one of the major parameters that determine the quantitative loading of the drug into the formulation. In the case of non-targeted liposomes %EE was slightly higher as compared to targeted

liposomes. That might be due to the loss of drugs during the process of making targeted formulation. However, the minor change in %EE did not significantly affect the activity.

Table 4.4. Particle size, PI, zeta potential and % EE data of different liposomal formulations

Formulation type	Particle size (nm) (Mean±S.D*)	PI (Mean ±S.D*)	Zeta potential (mV) (Mean ±S.D*)	% EE (Mean ±S.D*)	DiD % EE (Mean ±S.D*)
Blank liposomes	144.3 ± 3.48	0.267 ± 0.78	-15.12 ± 0.70	-----	-----
RUT-LIPO	194.1 ± 4.12	0.159 ± 0.43	-21.53 ± 0.71	70.32 ± 2.43	-----
RGD-RUT-LIPO	218.3 ± 2.45	0.222 ± 0.12	-22.68 ± 1.43	68.98 ± 3.76	-----
ABX-RUT-LIPO	220. 2± 3.54	0.242 ± 0.04	-23.67 ± 1.94	67.67 ± 1.89	-----
DiD-LIPO	192.9 ± 5.28	0.200 ± 0.03	-21.68 ± 1.47	-----	62.64 ± 3.83
RGD-DiD-LIPO	224.5 ± 2.21	0.224 ± 0.08	-23.26 ± 2.87	-----	60.32. ± 1.79
ABX-DiD-LIPO	229.4 ± 2.60	0.287 ± 0.05	-23.43 ± 0.89	-----	61.58 ± 2.89

*n=3; S.D: standard deviation

4.5.2.3. SEM and TEM

The obtained SEM & TEM micrographs of RUT-LIPO, RGD-RUT-LIPO, and ABX-RUT-LIPO were depicted in **Figure 4.8A** (SEM) and **Figure 4.8B** (TEM). The morphological examination of the images revealed that the non-targeted liposomes and targeted liposomes were spherical in shape and were under the size range of 220 nm. The ring pattern in “selective area (electron) diffraction” (SAD or SAED) pattern analysis by TEM of liposomes was performed that are presented in **Figure 4.8C**. The SEM and TEM images in **Figure 4.8A** and **Figure 4.8B**. indicates that developed liposomes were uniformly dispersed, round in shape, and free from surface defects (cracks or pinholes). The average diameter of colloidal liposomes was in the range of 200 nm with a few of them having higher and lower size distribution Moreover, the minor increment in particle size was observed in the case of targeted formulation that was in absolute agreement with the particle size analyzer (DLS) value. Additionally the TEM images also suggesting that there was no leakage of drug or physical instability that leads to fusion or breakage of liposomes. The

SAED ring pattern analysis by TEM showed the amorphous nature (halo ring pattern) of all the liposomal formulations [219] (**Figure 4.8C**).

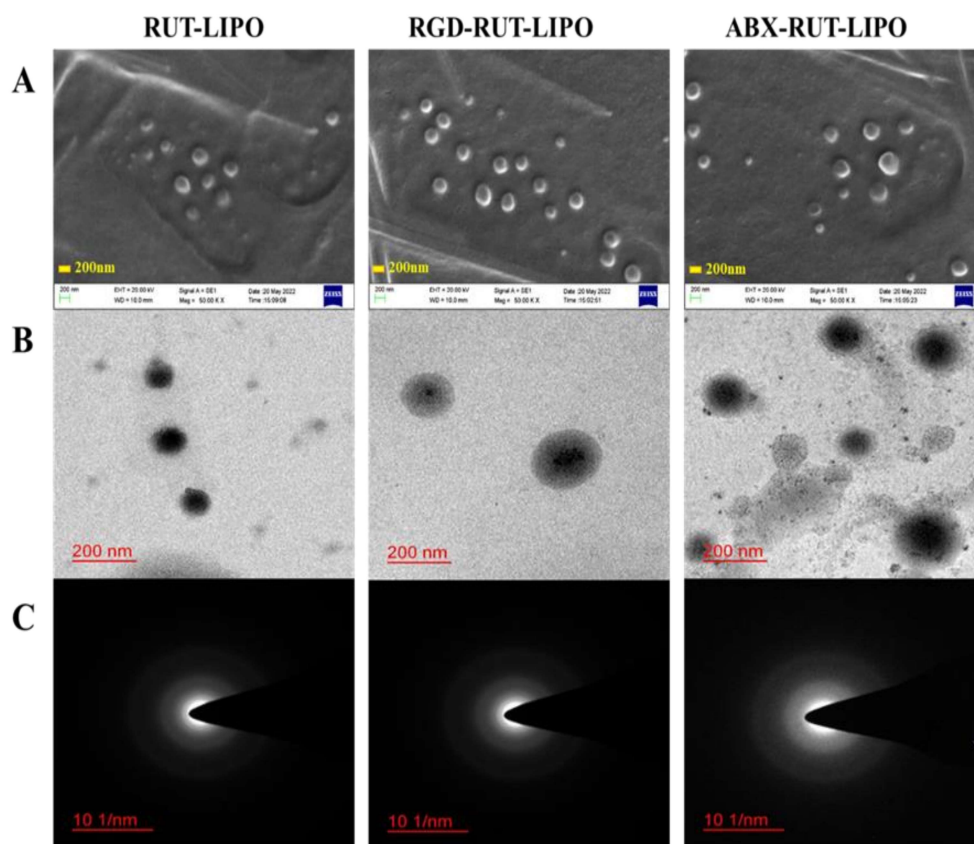


Figure 4.8. A) SEM images, B) TEM images, C) SAED pattern of RUT-LIPO, RGD-RUT-LIPO and ABX-RUT-LIPO

4.5.2.4. Bradford assay

The amount of conjugation for ABX and RGD on the liposomal surface, calculated by Bradford assay was found to be 64.76 ± 4.71 and 72 ± 7.56 % respectively in the targeted liposomes. Here % represents the amount of antibody or peptide conjugated with the –COOH group present on the surface of liposomes out of the total amount added initially. The RGD decorated liposomes showed higher conjugation than ABX conjugated liposomes, which could be due to the larger size of the monoclonal antibody that created

steric hindrance that restrict the surface binding. However, results suggested that the low conjugation of ABX did not impact the targeting ability of the liposomes.

4.5.2.5. Surface chemistry

The surface chemistry of non-targeted and targeted liposomes was investigated by XPS spectral analysis. As presented in **Figure 4.9A**, the XPS graph depicted peaks for components P, C, N, and O. The peaks obtained at binding energies 140-122, 291-277, 410-390, and 538-524 eV were denoted as P 2p, C 1s, N 1s, and O 1s. The percentage of P2p, C1s, N1s, and O1s in RUT-LIPO were 2.1%, 81.29 %, 2.28% and 12.48 % respectively, whereas, for RGD-RUT-LIPO, these were 1.7%, 81.20 %, 4.65 %, and 12.45 % and ABX-RUT-LIPO 1.81%, 79.21 %, 5.61 %, and 1.81% respectively. Moreover, the analysis of surface chemistry by high-resolution XPS was also carried out to confirm the conjugation of targeting moiety on liposomal surfaces. As compared to RUT-LIPO carbon's atomic % on the targeted liposomes was slightly lower revealing the coating of targeting moiety that covers the carbon backbone of liposomes. Whereas, nitrogen (N 1s) atomic % on RGD (4.65%) and ABX (5.61%) decorated liposomes significantly increased as compared to RUT-LIPO (2.28%). As the peptides and monoclonal antibodies have been reported as nitrogen-rich moieties, the increase in % nitrogen suggested the successful functionalization of the ABX/RGD on the surface of liposomal formulation (**Figure 4.9 B**). The atomic percentage of P2p was also observed to decrease in a targeted formulation that confirmed the HSPC constituted liposomes had been covered by surface conjugation. However, O1s atomic percentage did not show significant change which might be due to non-targeted liposomes being also oxygen-rich, the addition of targeting peptide covers that oxygen rich environment and replace the surface chemistry.

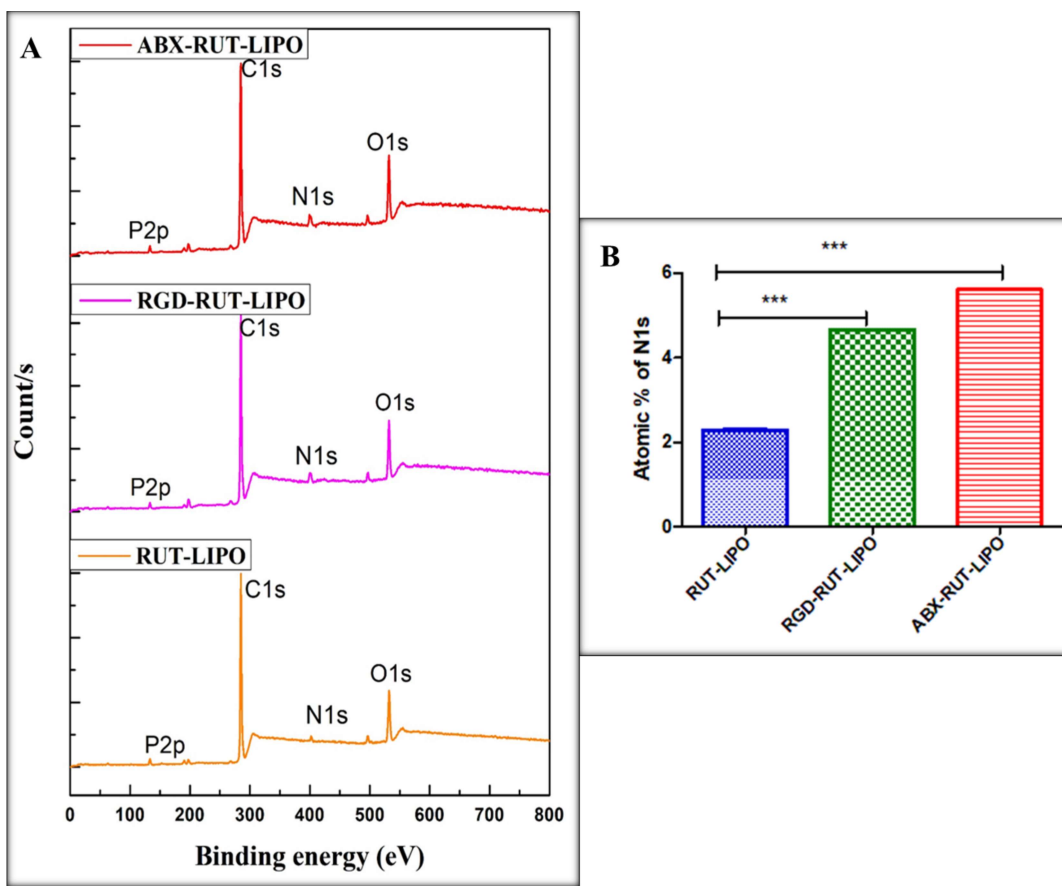


Figure 4.9. A) XPS survey of RUT-LIPO, RGD-RUT-LIPO and ABX-RUT-LIPO B) Bar graph of N1s atomic percentage in XPS spectra

4.5.2.6. XRD studies

Figure 4.10A showed the XRD overlay spectrum of optimized liposomal formulations with RUT. XRD spectrum of RUT showed sharp peaks at 2θ angles of 14.46° , 14.89° , 15.59° , 16.68° , 22.13° , 26.18° , and 26.75° . In the case of blank liposomes and RUT-LIPO, sharp peaks were observed at 31.54° and 66.10° . However, the XRD spectrum of targeted liposomes RGD-RUT-LIPO and ABX-RUT-LIPO-T2 contains a few extra peaks at 45.14° , 56.18° and 45.14° , 53.78° , 56.18° , 75.16° respectively. The XRD analysis of RUT discloses the crystalline nature with well-resolved peaks. Moreover, non-targeted and targeted liposomes revealed numerous small diffuse peaks in their XRD diffraction patterns. The characteristic XRD peaks of RUT were absent in liposomal formulations which confirms the amorphous nature of RUT in liposomes that also meets with the

agreement of SAED pattern analysis. During the TEM analysis, SAED ring patterns were taken by focusing on a single liposome area where crystal impurities were absent. The peaks of RUT were totally dissolved in liposomal formulations that support the proper encapsulation of RUT into the liposomes. The appearance of diffraction peaks in RUT liposomes was from the other components of liposomes such as sodium chloride of buffer etc. Targeted liposomes had shown some extra peaks in comparison with non-targeted liposomes that confirm the presence of targeting moiety in the liposomal formulation.

4.5.2.7. TGA studies

To further evaluate the thermal stability of excipients of liposomes and RUT-LIPO in terms of weight change, TGA analysis was used. In this, the variation in the weight of samples over a range of temperatures was determined. The TGA plots of cholesterol, HSPC, RUT, TPGS, and RUT-LIPO were indicated in **Figure 4.10 B**, the primary decline in mass of the sample may be due to the evaporation of water in liposomal suspension and the second decline in mass shows the degradation of products [220]. In the case of RUT, 7.56% of initial weight loss was due to loss of RUT moisture content and was observed in the range of 45 to 140 °C. Then, between 250-335 °C there was a gradual loss of weight (36.65%) that continues to 500 °C where the total loss of weight was 51.19%. As for RUT-LIPO, weight loss was observed in only one decline phase in a progressive manner in the range of 225-412 °C. Other excipients such as HSPC (307.40 to 364.19 °C), TPGS (346.19 to 432.40 °C) cholesterol (263.78 to 329.11 °C) showed an instant loss in weight in their first decline phase. The calculated percentage of weight loss revealed the feature of compound stability at a range of temperatures. RUT starts to lose its weight from 45 °C but when it was formulated as liposomes, degradation starts at 225 °C, which ensures the stability of RUT in the liposomal vesicle. The stability of other excipients such as HSPC, TPGS, and cholesterol was also observed to be improved as before formulating they were

showing a sharp decline in weight loss but when it was formulated as RUT-LIPO the weight loss was observed in a progressive manner at a wide range of temperatures (**Figure 4.10 B**) [221].

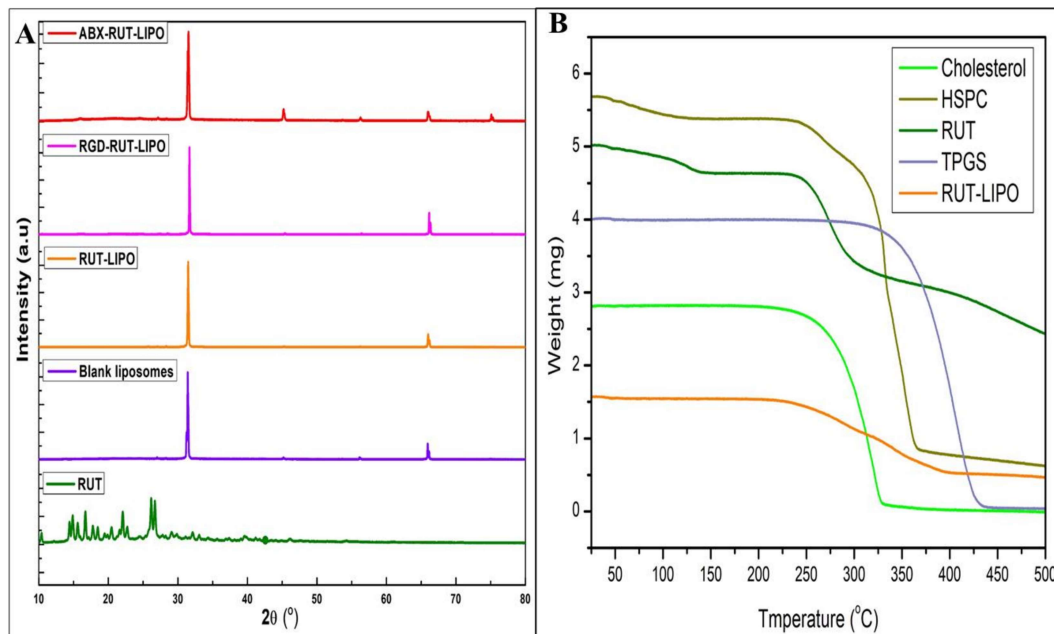


Figure 4.10. A) XRD spectra overlay of RUT, non-targeted and targeted liposomes B) TGA spectra of cholesterol, HSPC, RUT, TPGS, and RUT-LIPO

4.5.3. *In-vitro* studies

4.5.3.1. *In-vitro* drug release study

The *in-vitro* drug release of RUT, non-targeted, and targeted liposomal formulations were performed by dialysis method in pH 7.4 PBS. The cumulative release profiles of RUT, RUT-LIPO, RGD-RUT-LIPO, and ABX-RUT-LIPO liposomes in buffer (pH 7.4) were depicted in **Figure 4.11 A**. The percentage release was found to be 83.06 ± 1.11 %, 75.50 ± 0.81 %, and 78.62 ± 1.54 % for RUT-LIPO, RGD-RUT-LIPO, and ABX-RUT-LIPO liposomes respectively after 72 h of dialysis. However, over 99% of drug release was observed for RUT in 18h. The cumulative % drug release of RUT-LIPO was higher than the RGD-RUT-LIPO and ABX-RUT-LIPO at 72h time point. A sustained mode of RUT

release from targeted liposomes than non-targeted liposomes was noted without any signs of burst release for about 72 h. However, the RUT showed ~99% of release at 18 h.

4.5.3.2. Blood clot analysis

In-vitro assessment of antithrombotic activity of RUT, non-targeted, and targeted liposomes was performed by blood clot assay for determining clot inhibition efficiency as presented in **Figure 4.11 B**. The % blood clot formation values observed for BLN-RGD-LIPO, BLN-ABX-LIPO, RUT, RUT-LIPO, RGD-RUT-LIPO, and ABX-RUT-LIPO were 93.00 ± 2.94 , 90.22 ± 1.23 , 56.36 ± 5.83 , 48.26 ± 5.89 , 45.73 ± 5.30 , and 37.3 ± 5.93 % respectively (**Figure 4.11 C**). Targeted liposomes demonstrated a potent antithrombotic activity as compared to RUT, and RUT-LIPO. The % of a formed blood clot in the case of targeted liposomes was less than non-targeted liposomes due to the interaction of ABX or RGD on the surface of liposomes that offers specific binding to GPIIb/IIIa receptors as compared to free RUT.

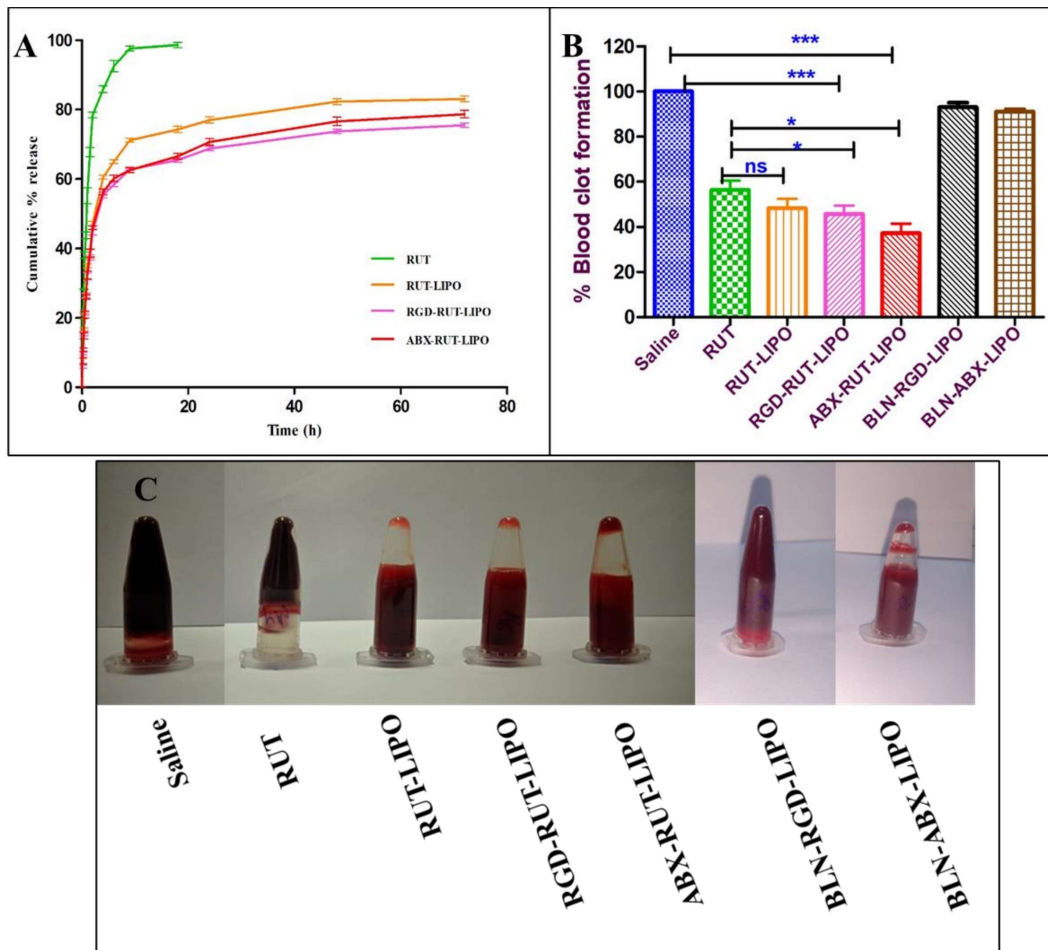


Figure 4.11 A) *In-vitro* drug release study of RUT and liposomes B) Bar graph representing %blood clot formation. C) Blood clot assay of non-targeted and targeted liposomes

4.5.3.3. *In-vitro* coagulation aPTT and PT assay

Evaluation of coagulation time is one of the fundamental studies to investigate the antithrombotic activity of a drug and drug products. In this study, the *in-vitro* aPTT and PT were tested after 1 h incubation of human plasma with the different liposomal formulations. The aPTT and PT for the saline control group were 65.56 ± 7.47 and 16.53 ± 2.42 sec, respectively, as shown in **Figures 4.12A and 4.12B**. The aPTT for BLN-RGD-LIPO, BLN-ABX-LIPO, RUT, RUT-LIPO, RGD-RUT-LIPO, and ABX-RUT-LIPO were found as 74.72 ± 6.33 , 85.14 ± 4.27 , 89.35 ± 8.30 , 94.20 ± 8.42 , 108.83 ± 11.44 and 297.96 ± 5.51 sec respectively. In addition, the PT value was recorded as 19.81 ± 5.33 , 21.33 ± 1.58 , 26.66 ± 2.71 , 25.10 ± 3.27 , 44.73 ± 3.34 , and 300.3 ± 7.39 sec for BLN-RGD-LIPO, BLN-

ABX-LIPO, RUT, RUT-LIPO, RGD-RUT-LIPO, and ABX-RUT-LIPO respectively. Moreover, comparing the coagulation time of two groups, the saline, and the pure drug, limited differences in aPTT or PT results were found. This implied that the RUT exhibited limited anticoagulant activity as a pure drug. Despite that in comparison with saline, RUT, and RUT-LIPO, the PT and aPTT were observed longer for targeted liposomes, confirming their potent antithrombotic effect in both intrinsic and extrinsic coagulation pathways.

4.5.3.4. Platelet aggregation studies

The primary hemostasis starts with platelet aggregation by the attachment of fibrinogen with GPIIb/IIIa receptors. The process progressively allows other platelets to activate and bind with each other to form the aggregate. In this study, the inhibition efficiency for platelet aggregation was estimated to identify the therapeutic potential of prepared liposomes. It was observed that the BLN-RGD-LIPO, BLN-ABX-LIPO, and RUT plots showed maximum absorbance after 1-2 min of fibrinogen addition. However, RUT-LIPO, RGD-RUT-LIPO, and ABX-RUT-LIPO showed maximum absorbance after 10 min, 11 min, and 11 min respectively depicted in **Figure 4.12C**. It was noted that RUT has significant potential for prevention of the platelets aggregation but targeting moiety (RGD or ABX) on targeted liposomes amplifies its inhibitory activity and prevents clot formation more prominently compared with free RUT and non-targeted liposomes. In short, the platelet aggregation assay revealed the superior antithrombotic potential of ABX-RUT-LIPO over other liposomal formulations which could be due to the higher affinity of ABX to human integrin receptors.

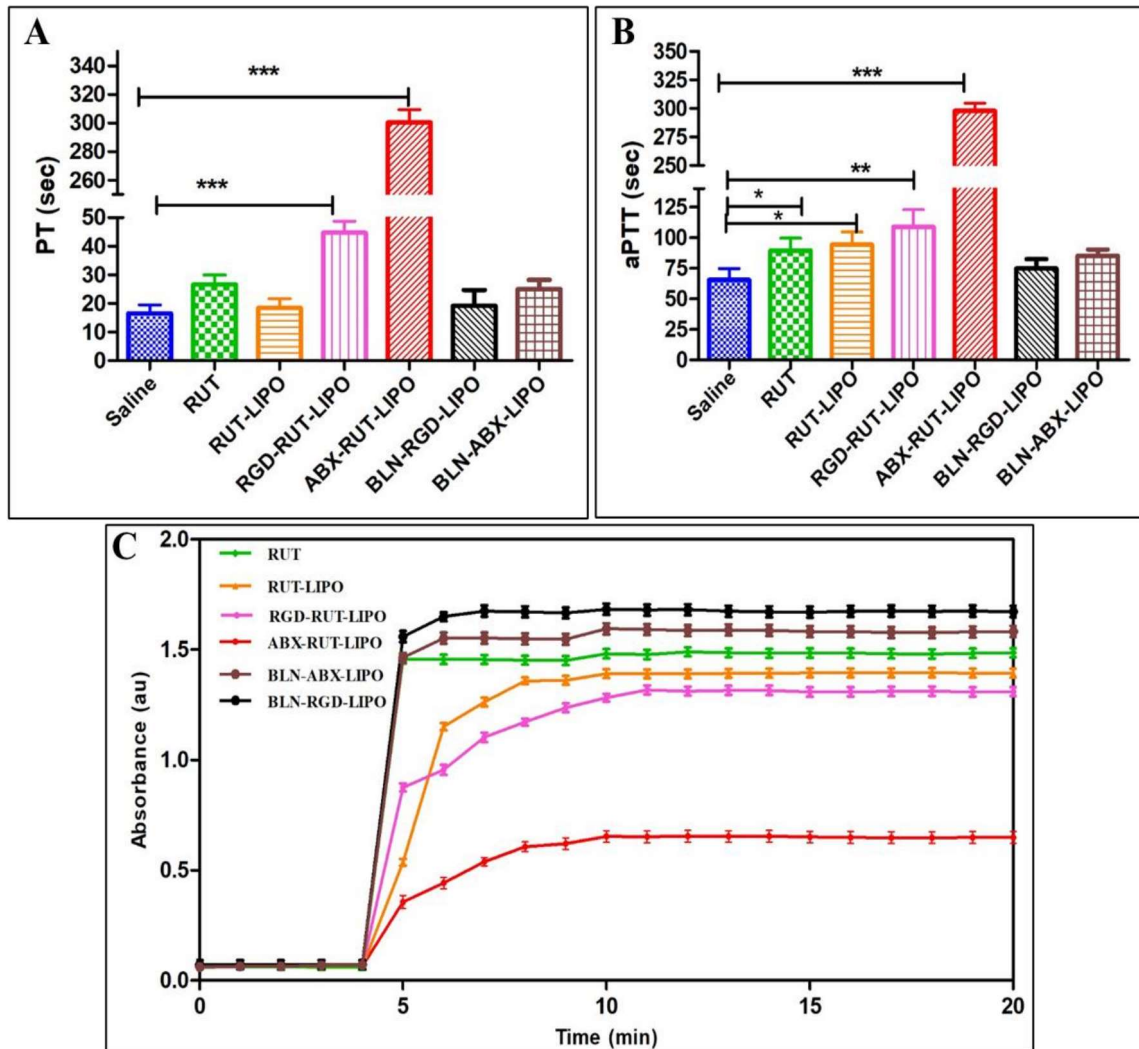


Figure 4.12. A) *In-vitro* PT in terms of time in sec has been presented B) *In-vitro* aPTT in terms of time in second has been presented for non-targeted and targeted liposomes, with saline as a positive control and RUT as a negative control. C) A plot of platelet aggregation study for the RUT, non-targeted and targeted liposomes

4.5.3.5. Biocompatibility and safety evaluation

4.5.3.5.1. Blood Smear

A biocompatibility study on human blood was performed by preparing a blood smear after incubation of liposomal formulations with human blood. All the pictures (Figure 4.13 A) of blood smear captured by bright-field microscope demonstrated blood cells retained their morphological structure after treatment with saline and liposomal

formulations. The blood smear did not show any morphological changes in blood cells *in-vitro*.

4.5.3.5.2. Hemolytic Assay

The biocompatibility and safety of the RUT-LIPO, RGD-RUT-LIPO, and ABX-RUT-LIPO in the human blood were investigated. The percentage of hemolysis for the RUT, RUT-LIPO, RGD-RUT-LIPO, and ABX-RUT-LIPO were found to be 0.35 ± 0.10 , 2.51 ± 0.81 , 2.64 ± 0.49 and 2.72 ± 0.75 %. The results presented in **(Figure 4.13 B)** demonstrated that all the liposomal formulations were non-hemolytic to human blood. In addition, the safety of the RUT-LIPO, RGD-targeted, and ABX-targeted liposomes in the human blood was demonstrated by the hemolytic study. The study demonstrated that none of the liposomal formulations showed more than 10% hemolysis and were biocompatible with human blood.

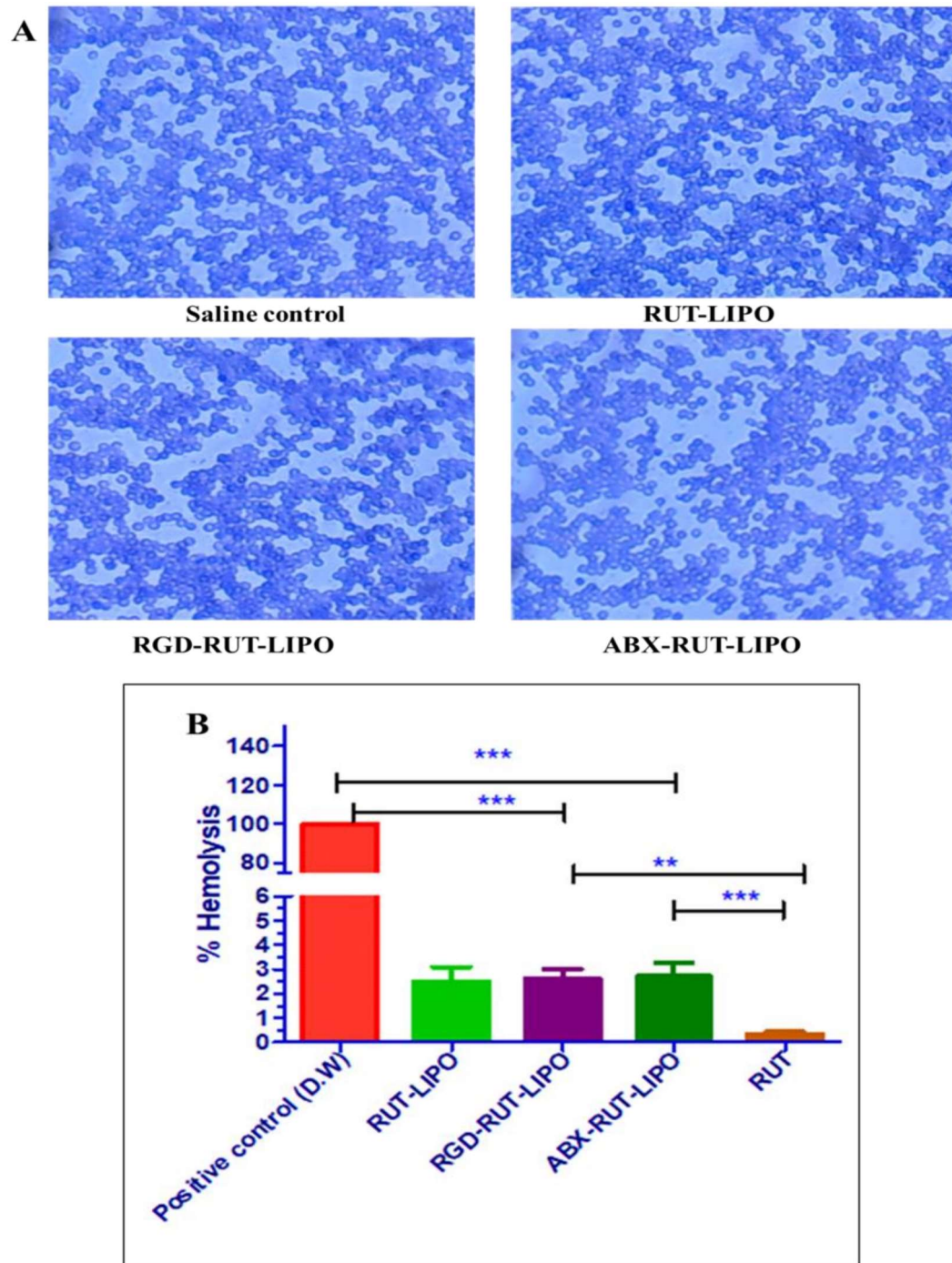


Figure 4.13. A) Bright microscopic images (10 X) and B) Percent hemolysis of human blood treated with saline, RUT, non-targeted, and targeted liposomes

4.5.3.6. *In-vitro* cytotoxicity assay

The cytotoxicity of prepared liposomes and RUT as drug control was investigated in the L929 mice fibroblast cells after 48 h incubation at 37 °C. The obtained results have been

depicted in **Figure 4.14**, which suggests that RUT elicits dose-dependent cytotoxicity, however, the liposomal formulations possess no significant cytotoxicity and were proven as cytocompatible in nature. Furthermore, the cytotoxicity performed on L929 mice fibroblast cells depicts the percent cellular viability of L929 fibroblast cells after 48 h treatment with BLN-LIPO, BLN-RGD-LIPO, BLN-ABX-LIPO, RUT control, RUT-LIPO, RGD-RUT-LIPO, and ABX-RUT-LIPO. The results obtained from cellular viability demonstrated that blank liposomes were nontoxic and did not show any significant reduction of cell viability when taken at the equivalent volume of the RUT loaded liposomes after 48h of treatment. However RUT was found to have concentration dependent cytotoxicity toward L929 cells, at 100 $\mu\text{g/mL}$ of RUT, viability was reduced up to ~84 %. However, in RUT loaded non-targeted and targeted liposomes, cellular viability was not affected significantly (~92% at 100 $\mu\text{g/mL}$); this may be due to the limited and sustained release of the RUT from liposomes. So the decrease in cell viability was observed due to the cytotoxicity of RUT, however, it was non-significant.

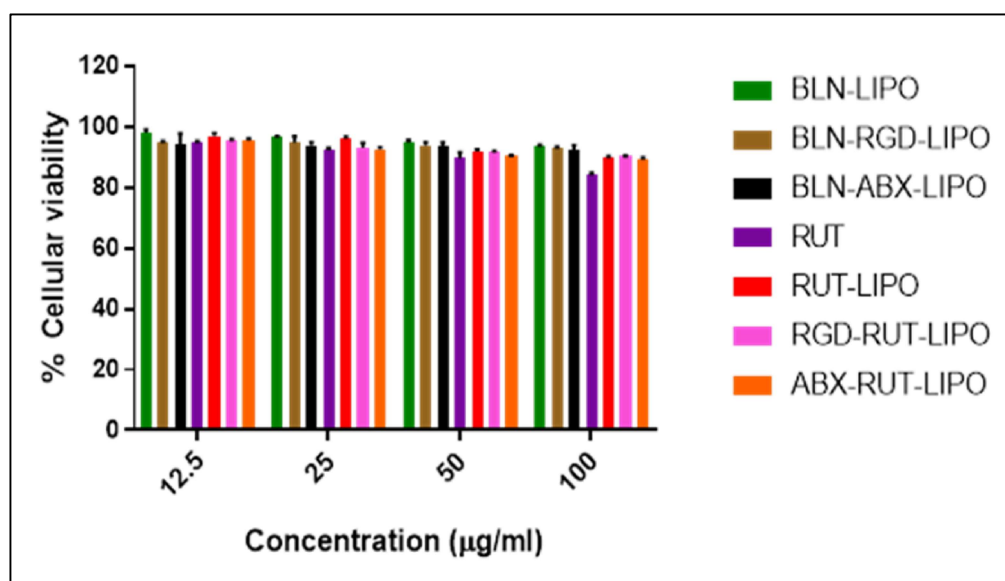


Figure 4.14. Cell cytotoxicity study of liposomal formulations in L929 fibroblast cell line

4.5.3.7. *In-vitro* clot targeting efficiency by platelet binding

4.5.3.7.1. *In-vitro* imaging

Platelet binding affinity was determined to obtain clot targeting ability of targeted liposomes against activated platelets. The bioluminescent signal from dispersed platelets in phosphate buffer saline incubated with DiD-LIPO, RGD-DiD-LIPO, and ABX-DiD-LIPO was captured by using photon imager optima and the value of ROI data (Radiance in p/sec/cm²/Sr) was noted as 28.47 ± 4.01 , 65.61 ± 4.74 and 93.70 ± 3.97 respectively, presented in **Figure 4.15A and 4.15 A.1**. The data displayed that platelets incubated with targeted liposomes exhibited a significantly higher intensity ($P < 0.05$) compared to the normal dye and the negative control. However, platelets treated with non-targeted liposomes had considerably lower intensity than targeted liposomes.

4.5.3.7.2. *Image-J* analysis of CLSM images

The *in-vitro* platelet binding affinity of DiD dye, non-targeted and targeted liposomes towards the activated platelets was determined by the use of Image J software. After the treatment intensity of red channels was estimated in obtained CLSM images. The captured images were processed into binary black and white images and a portion of the dark zone was quantified. Later, the fluorescent intensity of the red channel of the treated platelets was computed as 0.110 ± 0.016 , 0.155 ± 0.017 , 0.451 ± 0.021 , and 0.550 ± 0.026 for DiD dye, DiD-LIPO, RGD-DiD-LIPO, and ABX-DiD-LIPO respectively, had been presented in **Figure 4.15B and 4.15 B.1**. The higher fluorescent intensity was observed in the activated platelets after incubation with DiD loaded targeted liposomes as compared with free DiD dye and non-targeted liposomes. Further, it confirms the specific interactions of ABX or RGD of the targeted liposomes with the GP IIb / IIIa receptor of the activated platelets. Here, the fluorescent images color intensity was observed less as there was no cellular uptake although the images were higher magnification. The images show only the

surface binding of liposomal formulations over the activated platelets. The binary diagrams were used here for better visualization. This study was mainly designed to confirm the binding of liposomes at the targeted site.

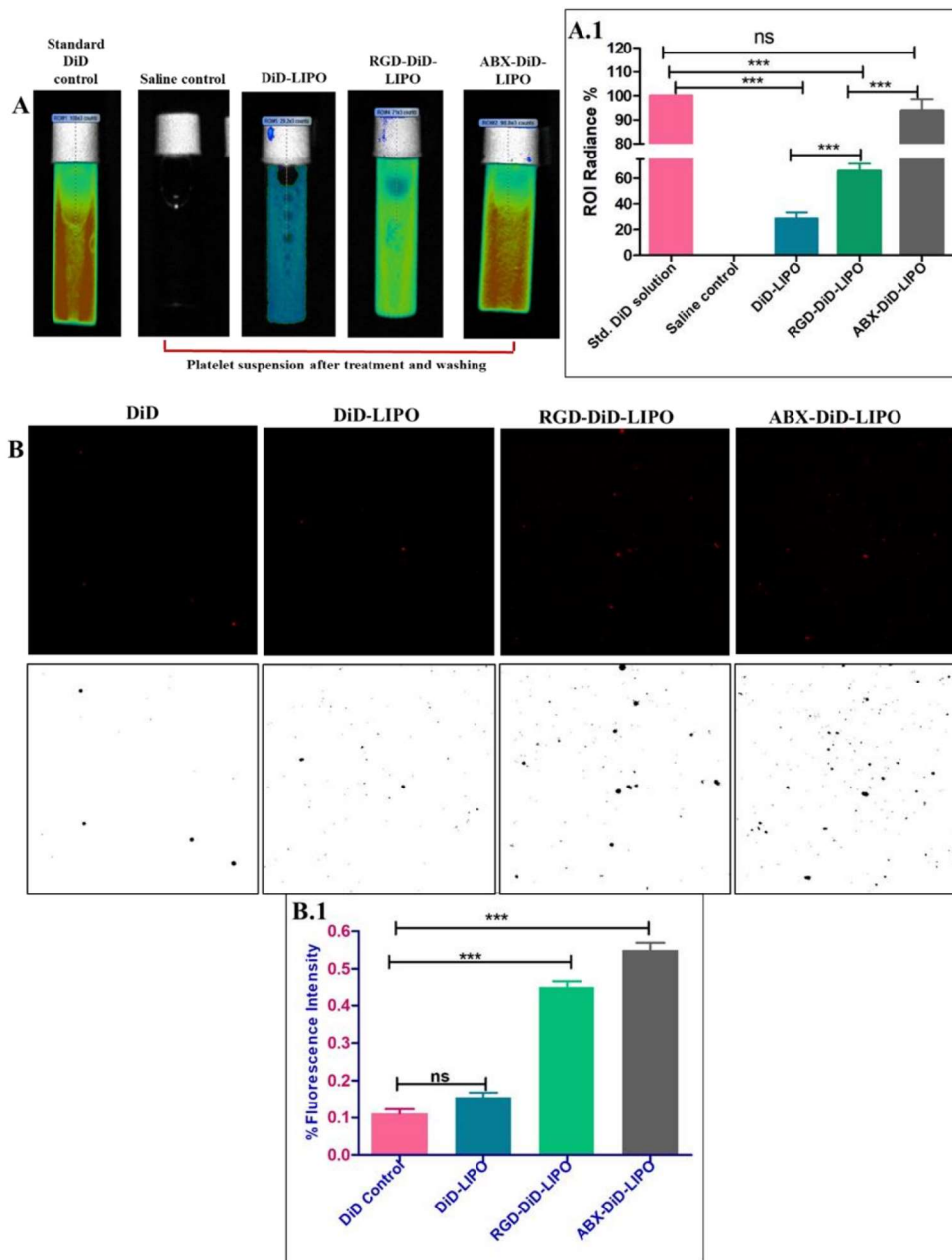


Figure 4.15. A) Bioluminescent images of vials containing activated platelets after the incubation with saline, DiD dye, non-targeted and targeted formulations. A.1) Graphical illustration of % interaction of non-targeted and targeted liposomes in comparison with DiD control; B) Fluorescent images and converted binary black and white images of activated platelets after treatment with DiD dye, non-targeted and targeted liposomes. B.1) Graphical representation of the % fluorescent intensity of red channels from CLSM images

4.5.3.8. Stability study

4.5.3.8.1. Serum stability study

The serum stability of RUT-LIPO was determined by comparing the size distribution spectra before and after incubation with 10% FBS that was recorded by a particle size analyzer. The size distribution curve of RUT-LIPO appeared as a single peak in the range of 30 to 650 nm in the analysis. However, FBS showed a double peak, first at 32-106 nm and second at 122-800 nm range. After incubation, the double peak was observed with no proper segregation in the range of 30-650 nm. The results were depicted in the plot in **Figure 4.16**. The results suggested a limited change in the size distribution of RUT-LIPO since the curve overlapped with each other without significant change, after and before incubation.

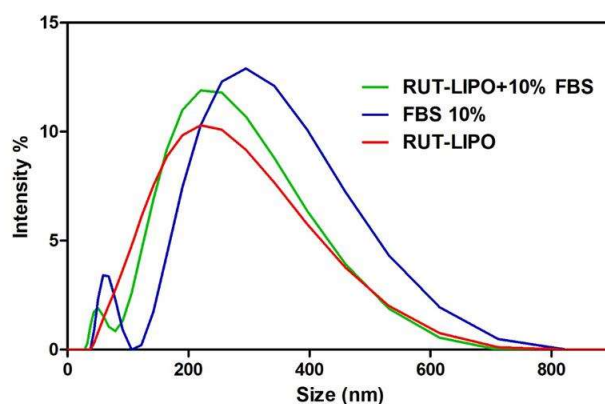


Figure 4.16. Stability study: size distribution of RUT-LIPO in 10% fetal bovine Serum.

4.5.3.8.2. Storage stability study

The stability study was performed to check the structural integrity and size of the prepared liposomal formulations. The result indicates no significant change in the size of RUT-LIPO, RGD-RUT-LIPO, and ABX-RUT-LIPO after storage of 3 months at 4-8 °C. The particle size and PDI data before and after storage was represented in **Table 4.5**. These findings confirm that liposomal formulation was stable and able to resist serum induced binding and aggregation.

Table 4.5. Stability of liposomes after and before 3 month of storage at 4-8°C in terms of size and PDI

Formulation type	Before storage		After storage	
	Particle size (nm) (Mean ± SD*)	PDI (Mean ± SD*)	Particle size (nm) (Mean ± SD*)	PDI (Mean ± SD*)
RUT-LIPO	209.90±2.39	0.254±0.015	212.36±3.00	0.261±0.005
RGD-RUT-LIPO	217.91±2.64	0.206±0.013	219.56±1.24	0.220±0.011
ABX-RUT-LIPO	223.43±1.69	0.284±0.021	225.03±2.59	0.263±0.020

*n=3

4.5.4. In-vivo studies

4.5.4.1. Tail bleeding assay

A tail bleeding assay was carried out on Swiss Albino mice to verify the antithrombotic efficacy of RUT-LIPO, RGD-RUT-LIPO, and ABX-RUT-LIPO liposomes. This assay was extensively used as an *in-vivo* method to determine bleeding related aspects of an antithrombotic drug and drug products. In this study, the bleeding time after the tail vein injection in the mice was measured. The bleeding time for saline, BLN-RGD-LIPO, BLN-ABX-LIPO, RUT, RUT-LIPO, RGD-RUT-LIPO, and ABX-RUT-LIPO were noted as 72.00±2.16, 68.66±3.85, 76.00±2.16, 112.00±2.16, 82.66±6.45, 85.33±1.24, and 88.66±3.85 sec respectively after 1 h of the injection. The method and bar graph of comparative bleeding time was presented in **Figure 4.17 A, B and C**. The liposomal formulations did not show any significant bleeding at lower dose in comparison to free RUT. The non-specific interactions of RGD and abciximab with platelets were reduced for targeted liposomes as a lower quantity of targeting peptide was used. The RUT showed higher bleeding as it is freely available in systemic circulation after 1 hr of i.v injection, the drug release data showed 55.18±3.22 % of RUT release after 1 h of dialysis. However, the liposomal formulations RUT-LIPO, RGD-RUT-LIPO, and ABX-RUT-LIPO showed 38.48±1.69%, 32.03±1.42%, and 32.28±1.63% of drug release after 1h of dialysis that

allow controlled release of RUT that helps to reduce the bleeding complications. From the above mentioned results, it was concluded that both the targeted liposomal formulation showed no significantly different bleeding time that corresponds to their specificity towards the thrombotic event and enhanced antithrombotic potential *in-vivo* without increasing bleeding risk.

4.5.4.2. Blood clotting time study

A clotting time study was performed on male swiss albino mice to investigate the anticoagulant effect of RUT and other liposomal formulations. The clotting time signifies the time required to generate thrombin to stop the bleeding. The clotting time for saline, BLN-RGD-LIPO, BLN-ABX-LIPO, RUT, RUT-LIPO, RGD-RUT-LIPO, and ABX-RUT-LIPO were noted as 121.00 ± 8.04 , 134.66 ± 4.02 , 134.66 ± 9.46 , 176.00 ± 4.32 , 146.33 ± 14.65 , 151.00 ± 9.93 and 149.00 ± 12.32 sec respectively after 1 h of the intravenous injection. The bar graph representing comparative clotting time was depicted in **Figure 4.17 D**. In comparison to RUT control, other liposomal formulations showed a reduced clotting time that suggests they minimized the adverse effects associated with RUT and were proven as a good nanocarrier to deliver RUT.

4.5.4.3. FeCl₃ model for thrombus formation by B.P. measurement

An *in-vivo* study on Sprague Dawley rats was done to confirm the antithrombotic efficiency of non-targeted and targeted liposomes. Initially, after the right carotid artery cannulation, Whatmann paper saturated with 20% FeCl₃ solution was applied to the carotid artery in rats, till the complete occlusion. Time taken to decline by 50% in B.P (T₅₀) was measured with the help AD instrument. The T₅₀ for saline, BLN-RGD-LIPO, BLN-ABX-LIPO, RUT, RUT-LIPO, RGD-RUT-LIPO, and ABX-RUT-LIPO were observed as 3.56 ± 1.02 , 8.66 ± 1.24 , 9.93 ± 1.34 , 12.6 ± 2.26 , 20.1 ± 4.41 , 145 ± 8.30 , and 135.94 ± 44.04 min, respectively, were depicted in **Figure 4.17 E and F**. As compared to saline, and RUT-LIPO

formulations the targeted formulations showed a significantly higher value (time taken for clot formation) presented in **Table 6**. BLN-RGD-LIPO, and BLN-ABX-LIPO were included as a control in *in-vivo* studies, and they did not show any significant effect as it contains lower quantities of abciximab or RGD. Although the *in-vitro* antithrombotic potential was found superior in the case of ABX-RUT-LIPO but in this *in-vivo* rat model, it shows slightly lesser activity than RGD-RUT-LIPO which can be due to the moderate affinity of ABX towards rat integrin receptors [222]. Moreover, to confirm the impact of liposomal formulation on blood viscosity after i.v. administration, the B.P. of the rat was monitored before and after liposomal injection. The B.P. was stable with a mean B.P. of 93-95 mmHg and did not show any significant change that suggests the viscosity of blood was not affected after liposomal injection.

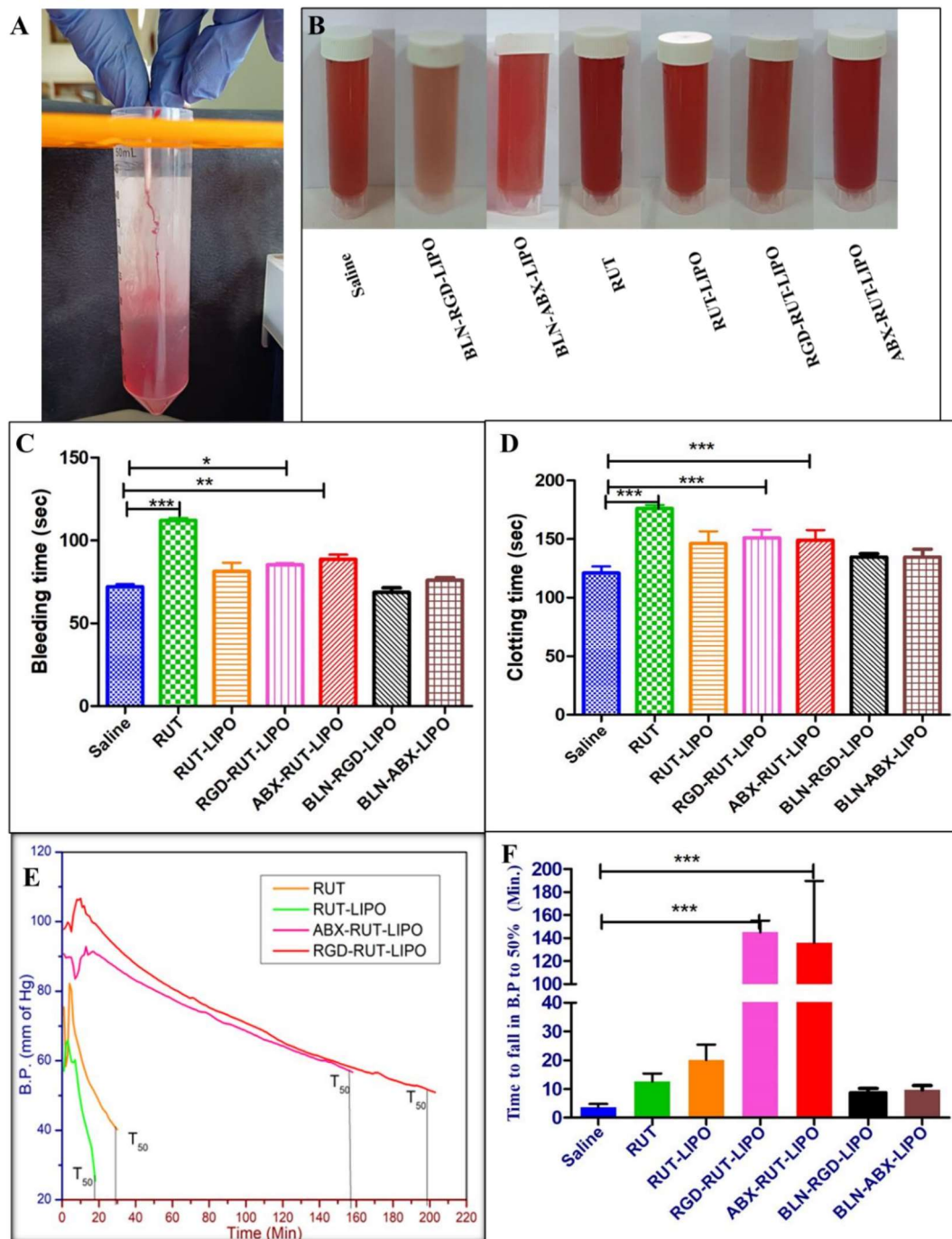


Figure 4.17. A) Tail bleeding assay in mice B) red intensity of blood of saline, BLN-RGD-LIPO, BLN-ABX-LIPO, RUT solution, non-targeted, RGD targeted, and ABX-targeted liposomes after tail bleeding C) Bar graph representing bleeding time in sec. D) Bar graph depicting the clotting time in sec. E) Line graph showing the original B.P. measurements F) Effect of various liposomal formulations on FeCl₃ induced blockage in CA blood flow. Bar diagram represents the time of 50% fall in B.P. of CA.

Table 4.6. Effect of various formulations on blood pressure in FeCl₃ induced blockage in CA

Group name	B.P. before treatment	B.P. after treatment	Avg time taken to fall in 50%
	(mm of Hg) (Mean ± SD#)	(mm of Hg) (Mean ± SD#)	B.P. (min) (Mean ± SD#)
Saline	93.33 ± 8.05	46.66 ± 4.02	3.56 ± 1.02
RUT	99.00 ± 6.48	49.50 ± 3.24	12.60 ± 2.26* (P<0.05)
RUT-LIPO	88.00 ± 5.71	44.00 ± 2.85	20.10 ± 4.41*
RGD-RUT-LIPO	101.33 ± 7.31	50.66 ± 3.65	145.00 ± 8.30*** (P<0.001)
ABX-RUT-LIPO	93.16 ± 8.46	46.58 ± 4.23	135.94 ± 34.04***
BLN-RGD-LIPO	92.00 ± 7.11	46.00 ± 3.55	8.66 ± 1.24 ns
BLN-ABX-LIPO	99.66 ± 4.10	49.83 ± 2.05	9.93 ± 1.34 ns

Values represent Mean ± S.D, *p < 0.05, **p < 0.01 and ***p < 0.001.

4.5.4.4. Pharmacokinetic study

In-vivo pharmacokinetic study of RUT, RUT-LIPO, RGD-RUT-LIPO and, ABX-RUT-LIPO were performed on male Sprague rats. The plasma RUT concentration versus time plot was obtained after i.v. administration of formulations at 5 mg/kg equivalent concentrations of RUT and depicted in **Figure 4.18**. The results demonstrated ~3 times higher relative bioavailability of RUT-LIPO, RGD-RUT-LIPO, and ABX-RUT-LIPO in comparison with RUT control. The pharmacokinetic parameters were presented in **Table 4.7**. The pharmacokinetic profile of RUT-LIPO, RGD-RUT-LIPO, and ABX-RUT-LIPO demonstrated improved half life and mean residence time as compared to RUT control (p < 0.05). Additionally, the liposomal formulations were depicted to have significantly lower clearance compared to RUT control. The enhancement in the mean residence time and increased plasma half life of RUT in the liposomal formulation may be due to the stealth effect of the liposomes on the encapsulated RUT. Further, the liposomal formulation was found to have lower V_d compared with free RUT, suggesting that liposomes were mainly constrained in the systemic circulation for a more extended period of time and thus available for producing antithrombotic effects for a prolonged period. The pharmacokinetic parameters were presented in **Table 4.7**.

(Selectivity: The selectivity of the method for the targeted analyte in the blank mobile phase and blank plasma were investigated through the comparison of HPLC chromatograms.

Extraction efficiency: the extraction efficiency of standard rutin concentrations 800, 1000, and 2500 ng/mL were found as 94.51%, 93.33 and 90.95% respectively.

The linearity studies were conducted in the concentration range of 0.2 $\mu\text{g/mL}$ to 10 $\mu\text{g/mL}$ and the value of the co-relation coefficient was found to be 0.999.

The accuracy data was calculated at the concentration of 200, 800, and 2500 ng/mL and %bias was found to be -11.68, -0.20, and 3.60% respectively.

Precision: Three different concentrations were scanned on the same day and three consecutive days and %RSD was found to be less than 15% at all concentration levels.

Precision was analyzed in the concentration of 400, 1000, and 5000 ng/mL, and %RSD was found to be 4.02, 2.35, and 0.06 % respectively. Additionally, the LOD and LOQ of the developed analytical method for the targeted compound were found to be 3.20 and 9.69 respectively.)

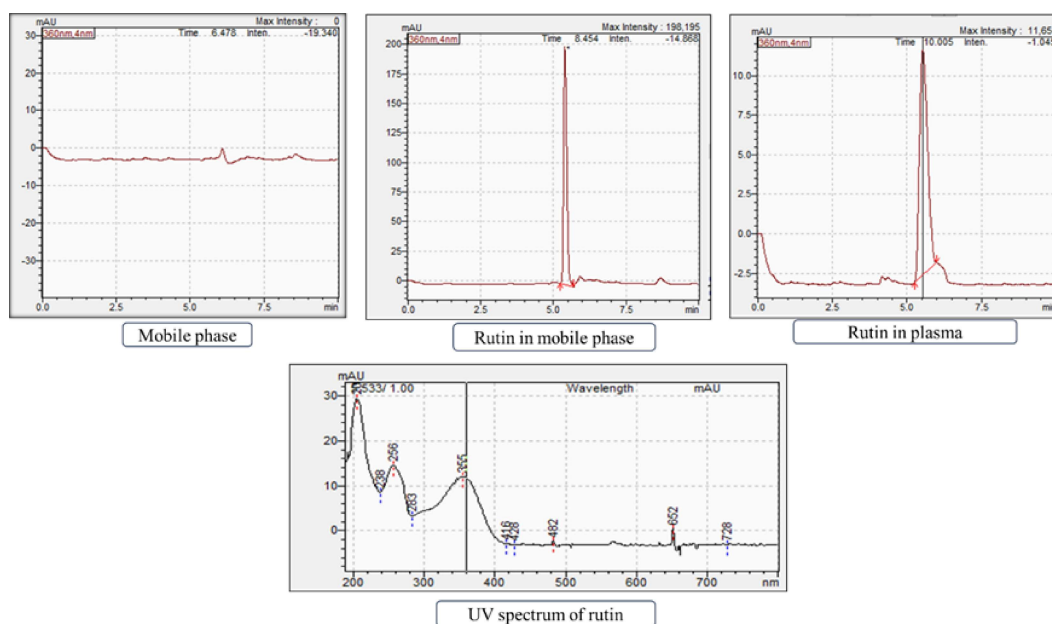


Figure 4.18. Chromatograms of analytical method development of rutin

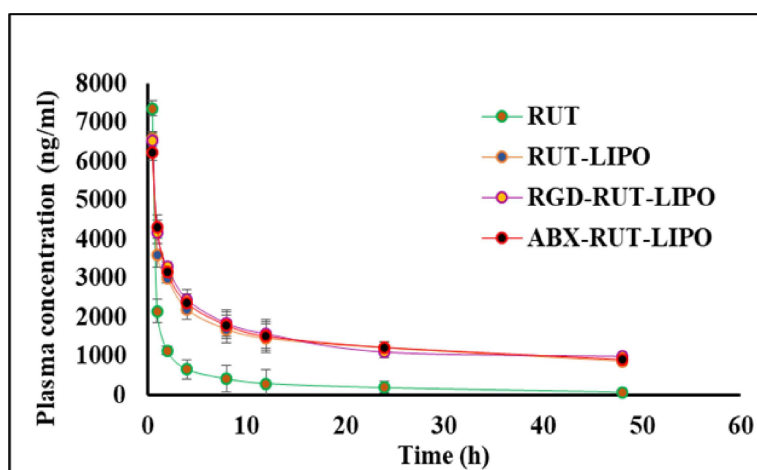


Figure 4.19. *In-vivo* pharmacokinetic study of RUT, RUT-LIPO, RGD-RUT-LIPO, ABX-RUT-LIPO after i.v. administration

Table 4.7. Pharmacokinetic parameters of RUT, RUT-LIPO, RGD-RUT-LIPO, and ABX-RUT-LIPO after i.v. administration at 5 mg/kg

Parameters	RUT (Mean \pm SD*)	RUT-LIPO (Mean \pm SD*)	RGD-RUT-LIPO (Mean \pm SD*)	ABX-RUT-LIPO (Mean \pm SD*)
AUC _{total} (ng.h/mL)	23427.27 \pm 1151.84	71146.34 \pm 1403.98	72133.47 \pm 1181.93	72690.25 \pm 1246.41
C _{max} (ng/mL)	7235.15 \pm 122.82	6499.75 \pm 73.83	6492.40 \pm 53.66	6257.42 \pm 78.70
T _{1/2} (h)	17.42 \pm 0.73	41.44 \pm 6.46	41.21 \pm 7.04	48.13 \pm 4.58
MRT (h)	12.04 \pm 0.47	54.72 \pm 8.61	57.13 \pm 8.68	64.38 \pm 5.61
V _d (L/kg)	1.01 \pm 0.04	0.49 \pm 0.03	0.46 \pm 0.04	0.51 \pm 0.03
Cl _{total} (mL/kg.h)	39.74 \pm 0.46	8.33 \pm 0.76	7.82 \pm 0.78	7.14 \pm 0.06
K _E (h ⁻¹)	0.040 \pm 0.002	0.017 \pm 0.003	0.017 \pm 0.003	0.015 \pm 0.002
F _R	-	3.04	3.08	3.10

*n = 3,

RUT: Rutin

RUT-LIPO: Rutin loaded liposomes.

RGD-RUT-LIPO: Rutin loaded RGD conjugated liposomes.

ABX-RUT-LIPO: Rutin loaded ABX conjugated liposomes.

MRT: Mean residence time.

V_d: Volume of distribution.

Cl_{total}: Total body clearance.

K_E: Elimination rate constant (fraction of drug in an animal that is eliminated per unit of time)

F_R: Relative bioavailability

4.5.4.5. Toxicity assay (histopathology study)

A histopathological study was executed to evaluate toxicity related to liposomal formulations, on vital organs in biological systems. The histopathological examination of different rat organs previously treated with liposomal formulation for the determination of the toxicity potential was performed by using a bright field microscope at 10X magnification. The liposomal formulation shows no significant toxicity *in-vivo* in rat brain,

heart, kidney, and liver showed in **Figure 4.19**. The result suggested no significant toxicity after i.v injection of liposomal formulation in 14 days. However few lesions were observed in cardiac tissue of the RUT group and in kidney tissue of the RUT-LIPO group but no toxicity was observed for targeted liposomal formulation.

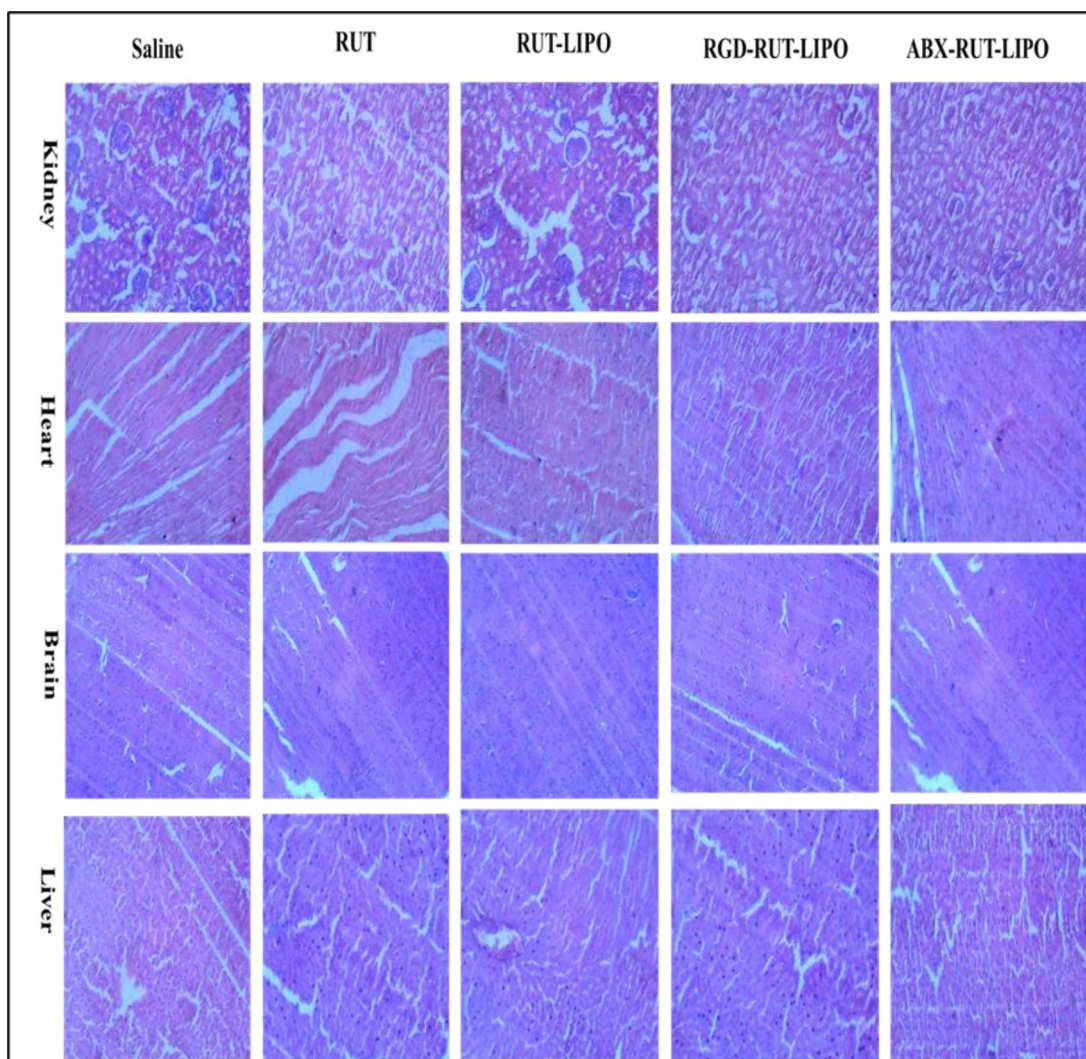


Figure 4.19. Histopathological examination of rat kidney, heart, brain, liver (H&E staining magnification 10X) after administration of saline, RUT, non-targeted, and targeted liposomes.

4.6. Conclusion

In this research, we proposed a novel liposomal formulation, which was loaded with RUT, and the surface of these vesicles was conjugated with tripeptide RGD and ABX

(monoclonal antibody) as a targeting moiety (antagonist of GP IIb/IIIa receptor) to target the thrombus site. The non-targeted and targeted liposomal formulations showed good stability, satisfiable hemocompatibility, better *in-vitro* and *in-vivo* efficacy as compared to pure drug. *In-vivo* evaluations demonstrated that RUT-LIPO, RGD-RUT-LIPO, and ABX-RUT-LIPO liposomal formulations maintained the antithrombotic function of RUT, prolonged the coagulation time in both intrinsic and extrinsic pathways. In comparison with RUT, RUT-LIPO solved the solubility, bioavailability, and short half-life problem of RUT, but minimized related side effects as well. Moreover, an *in-vitro* assessment carried out with human blood showed the more credible antithrombotic potential of ABX-RUT-LIPO over RGD-RUT-LIPO due to its crucial binding to human integrin receptors. However, the *in-vivo* assays executed on Sprague Dawley rats demonstrated slightly minimal antithrombotic activity of ABX-RUT-LIPO than RGD-RUT-LIPO implying the moderate targeting of ABX in rats. These thrombi targeted liposomal formulations had shown promising pre-clinical potential in thrombosis treatment, and after proper clinical investigations, it can be used for long-term antithrombotic therapy. As the large-scale production method of liposomes is already well established which might be an additional advantage of these liposomal vesicles.